Journal of Structural Geology 76 (2015) 1–21

Contents lists available at ScienceDirect

Journal of Structural Geology

journal homepage: www.elsevier.com/locate/jsg

# Factors controlling permeability of cataclastic deformation bands and faults in porous sandstone reservoirs

Gregory Ballas [a, b, *], Haakon Fossen [b, c], Roger Soliva [a]

[a] U.M.R. C.N.R.S. 5243 Géosciences Montpellier, University of Montpellier, UFR Sciences et Techniques, Place Eugène Bataillon, 34095 Montpellier Cedex 5, France
[b] Department of Earth Science, University of Bergen, Allégaten 41, N-5007 Bergen, Norway
[c] Museum of Natural History, University of Bergen, Box 7800, N-5020 Bergen, Norway

ARTICLE INFO

*Article history:*
Received 7 October 2014
Received in revised form
16 March 2015
Accepted 29 March 2015
Available online 18 April 2015

*Keywords:*
Cataclastic band
Permeability
Porous sandstone
Fluid flow
Tectonic regime
Burial depth

ABSTRACT

Improving the prediction of sub-seismic structures and their petrophysical properties is essential for realistic characterization of deformed sandstone reservoirs. In the present paper, we describe permeability contrasts induced by cataclastic deformation bands and faults in porous sandstones (766 data synthesized from field examples and the literature). We also discuss the influence of several factors, including tectonic regime, presence of a fault, burial depth, host sandstone porosity, and grain size and sorting for their initiation and permeability. This analysis confirms that permeability decrease is as a function of grain-crushing intensity in bands. Permeability reduction ranges from very limited in crush-microbreccia of compaction bands to high permeability reduction in cataclasites and ultracataclasites of shear-dominated bands, band clusters and faults. Tectonic regime, and especially normal-fault regime, with its tendency to localize strain and generate faults, is identified as the most important factor, leading to the formation of cataclastic bands with high permeability contrasts. Moreover, moderate burial depth (1–3 km) favors cataclastic bands with high permeability contrasts with respect to the host sandstone. High porosity, coarse-grain size and good grain sorting can slightly amplify the permeability reductions recorded in bands.



## 1. Introduction

Deformation bands are common features of sub-seismic scale structures developed in reservoirs composed of porous granular material such as sand and sandstone (Aydin and Johnson, 1978; Fisher and Knipe, 2001), carbonate grainstone (Tondi et al., 2006) or chalk (Wennberg et al., 2013). They accommodate mm- or cm-scale shear offsets, dilation or compaction (Aydin et al., 2006), and involve various micromechanisms of deformation, such as grain rearrangement (granular flow), cataclasis (grain cracking and comminution), or pressure-solution (Fossen et al., 2007 and references therein). In highly porous sandstone reservoirs, cataclastic bands showing a combination of compaction and shear are most common structures to result from localized deformation (Aydin, 1978; Underhill and Woodcock, 1987; Antonellini and Aydin, 1995; Wibberley et al., 2007; Tueckmantel et al., 2010). These structures can occur as individual strands, several tens of strands in tight deformation band zones or clusters, and generally occur around fault cores containing one or more localized slip-surfaces (e.g. Hesthammer and Fossen, 2001; Shipton and Cowie, 2001; Schueller et al., 2013 and references therein).

Cataclastic deformation bands can also be organized in pervasively distributed networks that appear not directly related to outcrop-scale faults (Solum et al., 2010; Saillet and Wibberley, 2010). In either case, they decrease porosity and permeability of the host sandstone (Fowles and Burley, 1994; Fisher and Knipe, 1998; Ogilvie and Glover, 2001; Fossen and Bale, 2007; Torabi et al., 2013). This decrease seems to be directly controlled by the intensity of cataclasis within the bands (Pittman, 1981; Crawford, 1998; Ballas et al., 2012). Cataclastic bands are therefore able to baffle or channelize fluid flow in reservoir settings (Harper and Moftah, 1985; Antonellini et al., 1999; Sternlof et al., 2006; Rotevatn et al., 2009; Tueckmantel et al., 2012). However, their quantitative and practical influence on reservoir performance remain unclear, and depends on both the geometry, distribution

* Corresponding author. Department of Earth Science, University of Bergen, Allégaten 41, N-5007 Bergen, Norway.
*E-mail address:* gregory.ballas@gm.univ-montp2.fr (G. Ballas).

http://dx.doi.org/10.1016/j.jsg.2015.03.013
0191-8141/

and petrophysical properties of the bands (Fossen and Bale, 2007; Brandenburg et al., 2012), of which the latter is the main focus of the present contribution.

Several factors influence the spatial distribution and petrophysical properties of cataclastic bands in porous sandstones (Schultz and Siddharthan, 2005; Fossen et al., 2007). Porosity, grain-size, grain sorting, grain shape, mineralogy, and lithification (mechanical compaction and cementation) represent internal sandstone characteristics controlling deformation initiation and mechanisms in porous and granular materials, whereas burial depth, tectonic regime and association with faults represent external controlling factors. Porosity determines the deformation behavior in granular material, from brittle regime and joint formation in low-porosity sandstone to macroscopically distributed ductile deformation and band development in high-porosity sandstone (Rutter, 1986; Wong et al., 1997; Du Bernard et al., 2002; Aydin et al., 2006; Rawling and Goodwin, 2006). Coarse grain-size favors initiation and localization of cataclastic bands (Schultz et al., 2010; Ballas et al., 2013) and seems to promote intense cataclasis (Chuhan et al., 2002; Balsamo and Storti, 2011). Good sorting (Antonellini and Pollard, 1995) and angular grain shape (Mair et al., 2002a) also promote cataclastic deformation. A high clay content favors disaggregation with the formation of phyllosilicate bands or clay smears (Fisher and Knipe, 2001; Fossen et al., 2007), whereas a large feldspar or lithic content promotes cataclastic processes (Antonellini et al., 1994; Chuhan et al., 2002; Rawling and Goodwin, 2003; Exner and Tschegg, 2012). Cementation may reduce sandstone porosity significantly, promoting brittle deformation (Swierczeska and Tokarski, 1998; Fisher et al., 2003; Balsamo et al., 2010). However, quartz-cemented sandstones with a high porosity are favorable sites for cataclasis (Johansen et al., 2005). Poor mechanical compaction or low packing density, increasing with burial depth, promotes diffuse grain rearrangement (Skurtveit et al., 2013) and the formation of disaggregation bands without any large change of permeability (Fossen, 2010), whereas compacted material favors cataclastic band formation (Kaproth et al., 2010; Kristensen et al., 2013). Burial depth also involves an increase in confining pressure, which may lead to more distributed deformation bands (Bésuelle, 2001; Mair et al., 2002b) and intense cataclasis (Antonellini et al., 1994; Crawford, 1998), and higher temperature, which promotes pressure-solution (Fisher and Knipe, 2001). Tectonic regime and presence of a large-scale fault also seem to influence the distribution of low-permeability cataclastic bands in porous sandstone reservoirs (Jamison and Stearns, 1982; Ballas et al., 2014), even if similar permeability reduction can be observed in bands formed in both normal- and thrust-fault regimes (Solum et al., 2010; Brandenburg et al., 2012).

Hence, several factors influence cataclastic band initiation and characteristics. However, influence on the permeability can be directly estimated for only few of them. A better knowledge of the relationships between the cataclastic band characteristics and factors influencing them is therefore necessary for understanding the influence of such sub-seismic structures on reservoir behavior. In the present paper, we analyze permeability contrasts induced by deformation bands and faults as a function of cataclasis intensity and discuss their potential control on fluid flow in porous sandstone reservoirs. To this end, we synthesized 766 permeability data of cataclastic bands and faults from literature (see Table 1, Table 2, and Supplementary Materials for spreadsheet) and new field examples (see Appendix for detailed description of these new data). We discuss also the influence of tectonic regime, presence of a large-scale fault, burial depth, and host sandstone porosity, grain size and grain sorting on this permeability contrasts induced by cataclastic deformation bands and faults in sandstone reservoirs. We believe that these data are representative for deformation band permeability in porous sandstone, at least for the factors discussed in the present contribution.

## 2. Methodology

The present paper is based on a synthesis of permeability data (766 data) from cataclastic deformation bands and faults formed in porous sandstone (Fig. 1). The major portion of these data is from the following references: Pittman (1981); Harper and Moftah (1985); Fowles and Burley (1994); Antonellini and Aydin (1994); Gibson (1998); Fisher and Knipe (1998); Ogilvie et al. (2001); Ogilvie and Glover (2001); Lothe et al. (2002); Shipton et al. (2002); Flodin et al. (2005); Keehm et al. (2006); Fossen and Bale (2007); Al-Hinai et al. (2008); Rotevatn et al. (2008); Torabi et al. (2008); Aydin and Ahmadov (2009); Torabi and Fossen (2009); Balsamo et al. (2010); Balsamo and Storti (2010); Medeiros et al. (2010); Solum et al. (2010); Tueckmantel et al. (2010); Balsamo and Storti (2011); Fossen et al. (2011); Sun et al. (2011); Tueckmantel et al. (2012); Ballas et al. (2013); Saillet and Wibberley (2013); Torabi et al. (2013); Ballas et al. (2014); Zuluaga et al. (2014) (see Tables 1 and 2). Previously unpublished permeability data from different sets of deformation bands in western US (Arches National Park, Buffington Windows, Pismo Basin, San Rafael Desert and San Rafael Reef) were also added to complete the data set, especially from structures formed in a thrust-fault regime (see Appendix). Only permeability data measured perpendicular to deformed bands are included in the present dataset.

Because the different methods of measurement introduce some variation in absolute permeability value (the TinyPerm permeameter, pressure-decay profile permeametry, air and nitrogen permeametry, numerical image analysis from thin-section or tomography, probe permeameter, Kozeny-Carman laws and more), we only considered the permeability contrast between the bands and faults vs. the host sandstones. The choice of methods for permeability quantification may also influence the permeability contrast value, but to a smaller extent. The *average value* ($\overline{X}$) of permeability contrast and the *standard deviation* were calculated for each type of cataclastic structures (from compaction band to fault core) and for each class defined according to factors such as tectonic setting, burial depth and host rock properties (for example, structures formed in coarse-grained sandstones being treated separately from structures formed in fine-grained sandstones). To limit the influence of the measurement variability between different studies, we used the average value for each study site in each paper (or each band set in the case of various band generations from the same site) for statistical analysis of external factors (tectonic regime, presence of fault and burial depth), and also for each host sandstone unit for statistical analysis of internal factors (porosity, grain size and sorting). We also calculated the minimum (*Min*) and the maximum (*Max*) permeability contrast for the different classes of bands relative to each factor.

All permeability data are plotted in Fig. 1. The proportion (%) of each type of cataclastic structure (from compaction band to fault core) was quantified for all defined classes with respect to the various factors. Graphs of distribution and frequency were extracted from this data set according to the different types of bands and factors. The proportion of bands inducing more than two orders of magnitude of permeability reduction was also calculated. Described as a permeability threshold between barrier and non-barrier structures for water flow under vadose conditions (Ballas et al., 2012), this proportion was used as a proxy to discuss the role of bands and related faults in reservoir behavior. We quantified also the proportion of sets containing bands involving permeability reductions greater than three orders of magnitude. This proportion

**Table 1**
Datasets used in this study (PCB: Pure Compaction Band; SECB: Shear Enhanced Compaction Band; CB: Cataclastic Band; ClB: Cluster Band; SlB: Slipped band; CCB: Cemented Cataclastic band; FC: Fault Core; Act: Actual burial depth; Max: Maximum burial depth; Band: burial depth at time of band formed).

| Source | Location | Number/type of data | Tectonic regime/Presence of fault | Burial depth (km) |
|---|---|---|---|---|
| Pittman, 1981 | Arbuckle Mountains (USA) | 17 (CB) | Normal/Yes | <1 (Act) |
| Harper and Moftah, 1985 | Gulf of Suez (Egypt) | 6 (CCB) | Normal (?) | 3.65 (Act) |
| Antonellini and Aydin, 1994 | Arches Park (USA) | 58 (ClB–FC) | Normal/Yes | ? |
| Fowles and Burley, 1994 | Scotland / England | 17 (CB–ClB) | Normal/Yes | 3 << 4 (Max) |
| Fisher and Knipe, 1998 | North Sea | 42 (CB–CCB – FC) | Normal/(?) | 0.5 << 3 (Act) |
| Gibson, 1998 | Various Sites | 8 (CB–ClB–CCB) | Various | >3 (Act) |
| Ogilvie et al., 2001 | Scotland | 4 (CB) | Normal/Yes | >1.5 (Max) |
| Ogilvie and Glover, 2001 | Scotland / North Sea | 6 (CB–CCB) | Normal/(?) | >1.5 (Max) |
| Shipton et al., 2002 | San Rafael Swell (USA) | 8 (CB–FC) | Normal/Yes | 1.5 << 3 (Max) |
| Lothe et al., 2002 | Norway | 7 (CCB) | Normal/Yes | ? |
| Flodin et al., 2005 | Valley of Fire (USA) | 16 (CB–FC) | Strike-Slip/Yes | <1.6 (Band) |
| Kheem et al., 2006 | Valley of Fire (USA) | 4 (SECB) | Reverse/No | <0.75 (Band) |
| Fossen and Bale, 2007 | Various Sites | 49 (CB–ClB) | Normal/Yes | ? |
| Al-Hinaï et al., 2008 | Moray Firth (Scotland) | 7 (FC) | Normal/Yes | >1.5 (Max) |
| Rotevatn et al., 2008 | Western Sinaï Peninsula (Egypt) | 14 (CB–SlB) | Normal/Yes | <1.5 (Max) |
| Torabi et al., 2008 | Various Sites | 18 (CB–CCB) | ? | ? |
| Aydin and Ahmadov, 2009 | Valley of Fire (USA) | 10 (PCB–SECB) | Burial/No | 2 < < 5 km (Band) |
| Torabi and Fossen, 2009 | San Rafael (USA) / Sinaï (Egypt) | 35 (CB) | Normal/Yes | Various |
| Balsamo et al., 2010 | Potiguar Basin (Brazil) | 8 (FC) | Normal/Yes | Shallow (Act/Max) |
| Balsamo and Storti, 2010 | Crotone Basin (Italy) | 34 (SECB–FC) | Normal (SS)/Yes | Shallow (Act/Max) |
| Medeiros et al., 2010 | Tucano Basin (Brazil) | 1 (ClB) | Normal/Yes | ? |
| Solum et al., 2010 | Buckskin Gulch / Big Hole (USA) | 30 (PCB–SECB–ClB) | Norm. –Rev./Yes–No | 1.5 << 3 (Max) |
| Tueckmantel et al., 2010 | Gulf of Suez (Egypt) | 34 (ClB–SlB) | Normal/Yes | 1.1 << 1.2 (Max) |
| Balsamo and Storti, 2011 | Crotone Basin (Italy) | 2 (FC) | Normal/Yes | 0.8 << 1 (Max) |
| Fossen et al., 2011 | Buckskin Gulch (USA) | 26 (PCB–SECB) | Reverse/No | <1.2 (Max) |
| Sun et al., 2011 | Valley of Fire (USA) | 1 (SECB) | Reverse/No | <0.75 (Band) |
| Ballas et al., 2012 | Provence (France) | 35 (CB–ClB – FC) | Normal/Yes | <0.4 (Max) |
| Tueckmantel et al., 2012 | Moray Firth (Scotland) | 3 (FC) | Normal/Yes | 1.8 (Act) |
| Ballas et al., 2013 | Provence (France)/USA | 24 (SECB) | Reverse/No | <0.8 (Max) |
| Saillet and Wibberley, 2013 | Provence (France) | 44 (CB–ClB – FC) | Norm. –Rev./Yes–No | 0.46 << 0.74 (Max) |
| Torabi et al., 2013 | Moab (USA) / Sinaï (Egypt) | 8 (CB–SlB) | Normal/Yes | 1.5 << 2.2 (Max) |
| Ballas et al., 2014 | Provence (France) | 22 (SECB–CB–ClB – FC) | Norm. –Rev./Yes–No | <1 (Max) |
| Zuluaga et al., 2014 | San Rafael Swell (USA) | 9 (CB) | Reverse/Yes | 2 << 2.8 (Max) |
| New data | San Rafael Reef (USA) | 27 (CB–SlB) | Reverse/Yes | 2 (Max) |
| | Arches Park (USA) | 15 (CB–ClB) | Normal/Yes | 2.5–3 (Max) |
| | San Rafael Desert (USA) | 22 (ClB–SlB) | Normal/Yes | 2<<3 (Max) |
| | Buffington Window (USA) | 74 (SECB) | Reverse/No | <1 (Band) |
| | Pismo Basin (USA) | 29 (CB–ClB–SlB) | Reverse/Yes | ? |

underlines the presence of potential barrier structures within an individual band set with bands of different permeability values (e.g. Tueckmantel et al., 2010).

## 3. Cataclastic deformation bands

Cataclastic deformation bands are characterized by grain cracking and comminution, a deterioration of grain sorting, an increase of grain angularity, and a reduction of host sandstone porosity by grain rearrangement and compaction (Sammis et al., 1987; Menéndez et al., 1996; Fossen et al., 2007). These textural changes promote strain hardening and leads to the progressive formation of band clusters that can precede the development of localized slip-surface(s) in fault zones (Aydin and Johnson, 1978; Mair et al., 2000). This progressive evolution of band organization at outcrop-scale is followed by an intensification of micro-scale cataclasis as a function of shear-offset along the bands (Engelder, 1974; Jamison and Stearns, 1982; Ballas et al., 2012). The degree of cataclasis can be classified using the terms crush microbreccia, protocataclasis, cataclasis and ultracataclasis, following the classification of Sibson (1977). The permeability of cataclastic deformation bands is expected to depend on the intensity of cataclasis (Crawford, 1998; Ballas et al., 2012; Torabi et al., 2013) which again varies for different kinds of band structures, and we decided therefore to classify the permeability data as a function of the different band structures as: (1) Pure compaction bands and Shear enhanced compaction bands, mostly composed of single-strands of crush microbreccia (Fig. 2i); (2) Cataclastic bands, which are formed by single or a few protocataclastic to cataclastic strands (Fig. 2ii); (3) Band clusters, consisting of several strands of cataclastic deformation (Fig. 2iii); (4) Slipped bands, showing cataclastic texture with an internal striated slip-surface (Fig. 2iv); and (5) Fault core, showing cataclastic to ultracataclastic texture along localized slip-surface(s) (Fig. 2v).

### 3.1. Pure and shear-enhanced compaction bands

Pure Compaction Bands (PCBs) and Shear-Enhanced Compaction Bands (SECBs) show an average permeability contrast of $-1.29 \pm 1.01$ (Fig. 2i). This contrast ranges from $-4$ to 1.1 with 15.3% of PCBs and SECBs having induced permeability reduction greater than two orders of magnitude. These bands show a very low degree of cataclasis (crush microbreccia), and seem incapable of forming barrier structures in a reservoir setting (e.g. Rotevatn et al., 2009). However, they can slightly altered reservoir flow patterns (Aydin and Ahmadov, 2009), introducing a gentle channelization of fluid flow (Sternlof et al., 2006) and increase flow tortuosity (Sun et al., 2011). Nevertheless, three sets out of 12 (25%) contain bands with permeability reduction greater than three orders of magnitude (Figs. 1 and 2i), but such PCBs and SECBs owe their reduction in permeability to both cataclasis and dissolution in the bands (Mollema and Antonellini, 1996; Fossen et al., 2011; Ballas et al., 2013) (See Fig. A2a, c in Supplementary Materials for examples of PCBs and SECBs showing both catacasis and dissolution processes).

**Table 2**
Additional characteristics for data sets used in this study (Sd: Sandstone; Qz: Quartz; Kaol: Kaolinite).

| Source | Name of formation/Diagenetic information | Porosity (%)/grain size (mm)/sorting of host rock | Method of permeability measurement |
|---|---|---|---|
| Pittman, 1981 | Simpson Group/Qz cement | 8.2/Fine/Poor | ? |
| Harper and Moftah, 1985 | Nubian Sd/Qz/Kaol cement | ?/Medium/Well | ? |
| Antonellini and Aydin, 1994 | Various Formations/? | 18 << 24/?/? | Mini permeameter |
| Fowles and Burley, 1994 | Penrith Sd/Qz cement | 14 << 25/Fine to Coarse/Well | Air Permeability (nitrogen) |
| Fisher and Knipe, 1998 | ? | ? | Water Flow permeability |
| Gibson, 1998 | Various/? | 4.3 << 23/?/? | Laboratory (Air??) |
| Ogilvie et al., 2001 | Hopeman Sd/Qz cement | 20/Fine to Medium/? | PDPK |
| Ogilvie and Glover, 2001 | Hopeman Sd/Qz cement | 7.5 << 21/Fine to Medium/? | ? |
| Shipton et al., 2002 | Navajo Sd/? | 24/Fine/Well | Probe Permeameter |
| Lothe et al., 2002 | Brumunddal Sd/Qz-Iron cement | 17 << 24/Fine to Coarse/Well | ? |
| Flodin et al., 2005 | Aztec Sd/Lithified | 15 << 25/Fine to Medium/Poor | ? |
| Kheem et al., 2006 | Aztec Sd/? | 15 << 25/Fine to Coarse/Poor–Well | Image Analysis |
| Fossen and Bale, 2007 | Various/? | ? | Tiny permeameter |
| Al-Hinaï et al., 2008 | Hopeman Sd/Qz cement | 10/Fine to Medium/Well | Flow Pump/Pulse Decay/Gas |
| Rotevatn et al., 2008 | Nubian Sd/Uncemented | 20 << 35/Medium to Coarse/Poor | Tiny permeameter and Gas |
| Torabi et al., 2008 | Entrada–Navajo–Nubian Sd/? | 21 << 31/Fine to Medium/? | Image Analysis |
| Aydin and Ahmadov, 2009 | Aztec Sd/Poorly-cemented | 21 << 25/Fine/? | Image Analysis |
| Torabi and Fossen, 2009 | Entrada–Nubian Sd/? | 26 << 30/Various/Poor–Well | Image Analysis |
| Balsamo et al., 2010 | Barreiras/Poorly lith. –Iron ce. | 1.7 << 6.8/Fine to Medium/Poor | |
| Balsamo and Storti, 2010 | ?/Poorly-lithified | ?/Fine to Coarse/Well | Tiny permeameter |
| Medeiros et al., 2010 | Ilhas Group/? | ?/Fine to Coarse/? | Tiny permeameter |
| Solum et al., 2010 | Navajo Sd/? | 20 << 24/Coarse/Well | Probe Permeameter |
| Tueckmantel et al., 2010 | Nubian Sd/Uncemented | 18 << 27/Medium to Coarse/? | Gas Permeameter |
| Balsamo and Storti, 2011 | ?/Poorly-lithified | ?/Fine–Coarse/Poor | Tiny permeameter |
| Fossen et al., 2011 | Navajo Sd/Poorly-cemented | 20 << 25/Coarse/Well | Tiny perm - Image Analysis - Gas |
| Sun et al., 2011 | Aztec Sd/Weakly-cemented | 18 << 20/Fine/Well | Image Tomography |
| Ballas et al., 2012 | Uchaux Sd/Uncemented | 27/Coarse/Poor | Gas Perm/Kozeny-Carman law |
| Tueckmantel et al., 2012 | Yellow Sd/No cement | 19 << 24/Fine to Medium/? | Gas Perm/Pulse Decay |
| Ballas et al., 2013 | Uchaux Sd/Uncemented | 17 << 39/Coarse/Poor | Kozeny-Carman law |
| Saillet and Wibberley, 2013 | Orange Sd/Uncemented | 29 << 30/Fine–Coarse/Well | Gas Permeameter |
| Torabi et al., 2013 | Entrada–Malha Sd/? | ?/Medium to Coarse/Well | ? |
| Ballas et al., 2014 | Various/Uncemented | 22 << 36/Fine–Coarse/Poor–Well | Kozeny-Carman law |
| Zuluaga et al., 2014 | Navajo Sd/Iron–Carb. cement | 20/Fine to Medium/Well | Tiny permeameter |
| New data | | | |
| San Rafael Reef (USA) | Entrada Sd/Poorly-cemented | 25 << 30/Fine/Well | Tiny permeameter |
| Arches Park (USA) | Entrada Sd/? | Various | Tiny permeameter |
| San Rafael Desert (USA) | Entrada Sd/Poorly-cemented | 25 << 30/Fine/Well | Tiny permeameter |
| Buffington Window (USA) | Aztec Sd/Poorly-cemented | 18 << 25/Coarse/? | Tiny permeameter |
| Pismo Basin (USA) | Edna Member/Oil field | 15 << 25/Medium to Coarse/? | Tiny permeameter |

### 3.2. Cataclastic bands

Cataclastic bands show an average permeability contrast of −1.67 ± 0.79 (Fig. 2ii). The contrast values range from −5.6 to 1 with 36.2% of cataclastic bands having induced permeability reduction greater than two orders of magnitude. A majority of sets (12 out of 20, ~60%) contain bands with large permeability reduction (greater than three orders of magnitude). Hence, these bands seem to be able to significantly reduce the permeability of the host sandstone reservoir (Figs. 1 and 2ii), and cataclastic band sets in reservoir settings should therefore have the capacity to impede fluid flow (Ogilvie et al., 2001), form local entrapments of fluid (Pittman, 1981), disturb reaction fronts (Taylor and Pollard, 2000) and increase flow tortuosity (Harper and Moftah, 1985). However, their real influence on production patterns depends directly on their spatial distribution and connectivity (Gibson, 1998), and it has been argued that variations in thickness and petrophysical properties along these bands prevent them from forming barrier structures (Fossen et al., 2007; Torabi and Fossen, 2009).

### 3.3. Band clusters

Cataclastic band clusters show an average permeability contrast of −2.65 ± 1.30 (Fig. 2iii). This contrast ranges from −6.5 to 0.1, with 61% of band clusters having induced permeability reductions greater than two orders of magnitude. A large majority of these bands strongly reduce the permeability of the host sandstone (Figs. 1 and 2iii) and 17 sets out of 23 (~74%) contain bands with large permeability reductions. These bands show intense cataclasis and seem to be able to affect reservoir transmissibility and impede fluid flow in sandstone reservoir (Antonellini and Aydin, 1994; Fowles and Burley, 1994; Ballas et al., 2014). However, similar to individual cataclastic bands, the large variations in thickness and petrophysical properties measured along cataclastic band clusters (Tueckmantel et al., 2010; Ballas et al., 2012; Rotevatn et al., 2013) and the preservation of interconnection within undeformed sandstone prevents them from fully compartmentalize sandstone reservoirs (Tindall, 2006; Medeiros et al., 2010).

### 3.4. Slipped bands

Slipped cataclastic shear bands show an average permeability contrast of −2.70 ± 0.97 (Fig. 2iv). This contrast ranges from −4.4 to −1.5 with 91.8% of slipped bands having induced permeability reduction greater than two orders of magnitude. Four sets out of 7 (~57%) have bands containing structures of large permeability reductions. They show intense cataclasis, largely reduce the permeability of the host sandstone reservoir (Figs. 1 and 2iv), and form potential permeability barrier for fluid flow (Fisher and Knipe, 1998; Tueckmantel et al., 2010). However, they are also prone to form preferential pathways for fluids parallel to the bands along their internal slip-surface(s) (Rotevatn et al., 2008; Torabi, 2014).

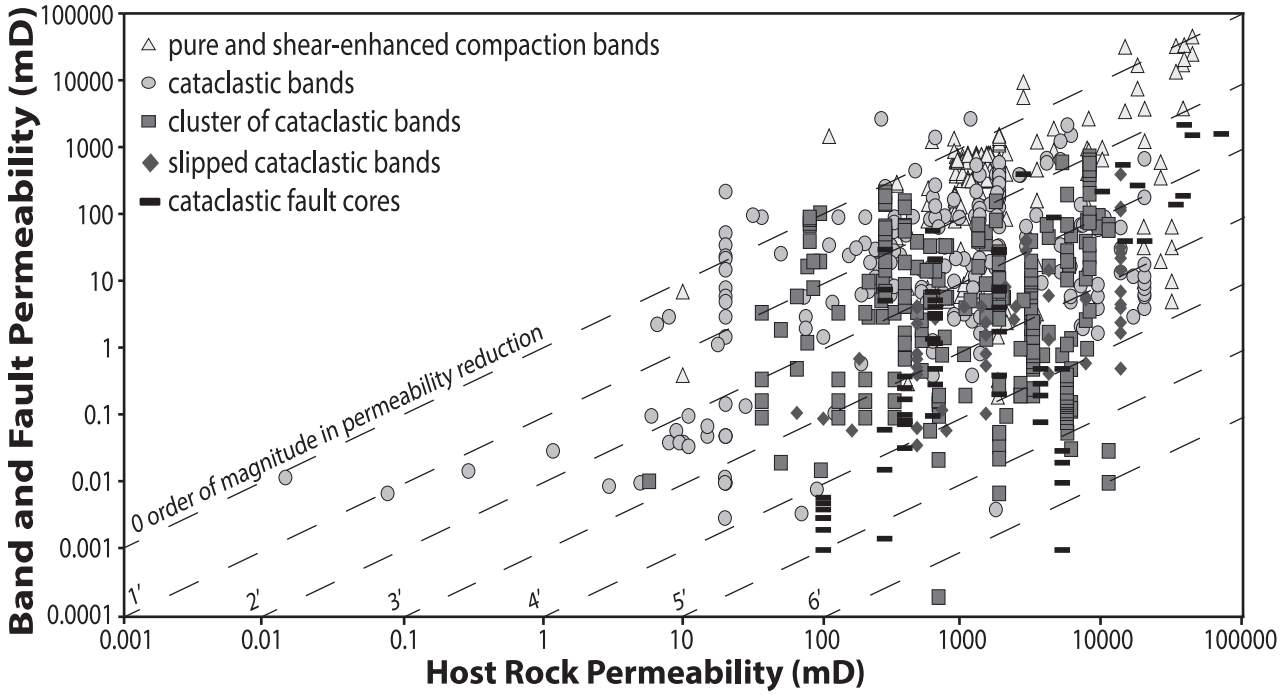


**Fig. 1.** Graph showing permeability values for various types of cataclastic deformation bands as a function of related host-sandstone permeability. These data come from 31 published studies and several new field examples (each dot represents a value of permeability measured on cataclastic structures and the corresponding permeability value of host rock which could be an average value on the study site) (See Table 1, Table 2 and Supplementary Materials).

### 3.5. Fault cores

Cataclastic fault cores show an average permeability contrast of −2.77 ± 1.29 (Fig. 2v). The contrast values range from −6.7 to 2 with 68.3% of fault cores having induced permeability reduction greater than two orders of magnitude. A large majority of these structures shows ultracataclastic texture (8 sets out of 11, ~73%) and largely reduces the permeability of the host sandstone (Figs. 1 and 2c). The presence of a single cataclastic fault core of low-permeability could therefore impede fluid flow to the same extent as distributed cataclastic deformation bands (Saillet and Wibberley, 2013; Torabi et al., 2013), compartmentalize gas reservoirs (Al-Hinaï et al., 2008; Tueckmantel et al., 2012), deviate groundwater flow in meteoric phreatic conditions (Balsamo et al., 2012), and reduce the reservoir transmissibility, although this behavior will depend on their continuity and shear displacement (Jourde et al., 2002; Shipton et al., 2002). Several cases of fault cores showing only moderate permeability are also reported by Balsamo and Storti (2010, 2011) and Torabi (2014) in porous sandstones and Balsamo et al. (2010) in iron-cemented sandstones, whereas the presence of cement within certain fault cores suggests preferential pathway for fluid flow during reactivation (Fowles and Burley, 1994; Ogilvie and Glover, 2001; Farell et al., 2014).

### 3.6. Comparison

A wide range in permeability contrast is observed for deformation band structures, and we see a progressive increase in permeability reduction from crush microbreccia of PCBs and SECBs to cataclasites/ultracataclasites of band clusters, slipped bands and fault cores (Figs. 2 and 3). Similarly, the maximum permeability contrast, the proportion of bands involving more than two orders of magnitude in permeability reduction, and the proportion of sets containing bands of large permeability decrease (greater than three orders of magnitude) increase progressively with the intensification of cataclasis within the bands. Based on these findings, structures potentially acting as baffles or seals in sandstone reservoirs would be structures with large shear/compaction ratio (greater than 7, Soliva et al., 2013), such as band clusters and localized faults (Fig. 3). The understanding of all factors controlling the type of cataclastic bands, shear localization, cataclasis intensity and permeability reduction, is necessary to realistically predict fault seal potential in porous sandstone reservoirs.

## 4. Tectonic regime and presence of fault

Permeability data of cataclastic deformation bands and faults were classified according to their kinematic behavior during formation: (1) in the normal-fault regime, (2) in the thrust-fault regime, and (3) in areas related to the presence of large-scale fault, i.e. bands located within fault damage zones above propagation of a basement fault, or in any band sets regionally linked to a fault, or (4) in areas devoid of fault (Fig. 4 and Table 1). The strike-slip regime was not investigated because of the limited amount of data available for this tectonic regime (Flodin et al., 2003; Saillet and Wibberley, 2013; Balsamo et al., 2013). See Supplementary Materials for detailed information (Fig. A1).

### 4.1. Normal-fault regime

Cataclastic structures formed in the normal-fault regime show an average permeability contrast of −2.30 ± 1.34 (Fig. 4a). This contrast ranges from −6.7 to 1.1, with 56.9% of normal-sense bands having induced permeability reduction greater than two orders of magnitude (Fig. 4a). Most sets (28 sets out of 42, ~67%) show normal-sense bands with structures involving large permeability decrease (greater than three orders of magnitude). Bands recorded include 4.8% as bands of low-intensity cataclasis, 34.9% as cataclastic bands, 36.2% as band clusters, 9.3% as slipped bands and

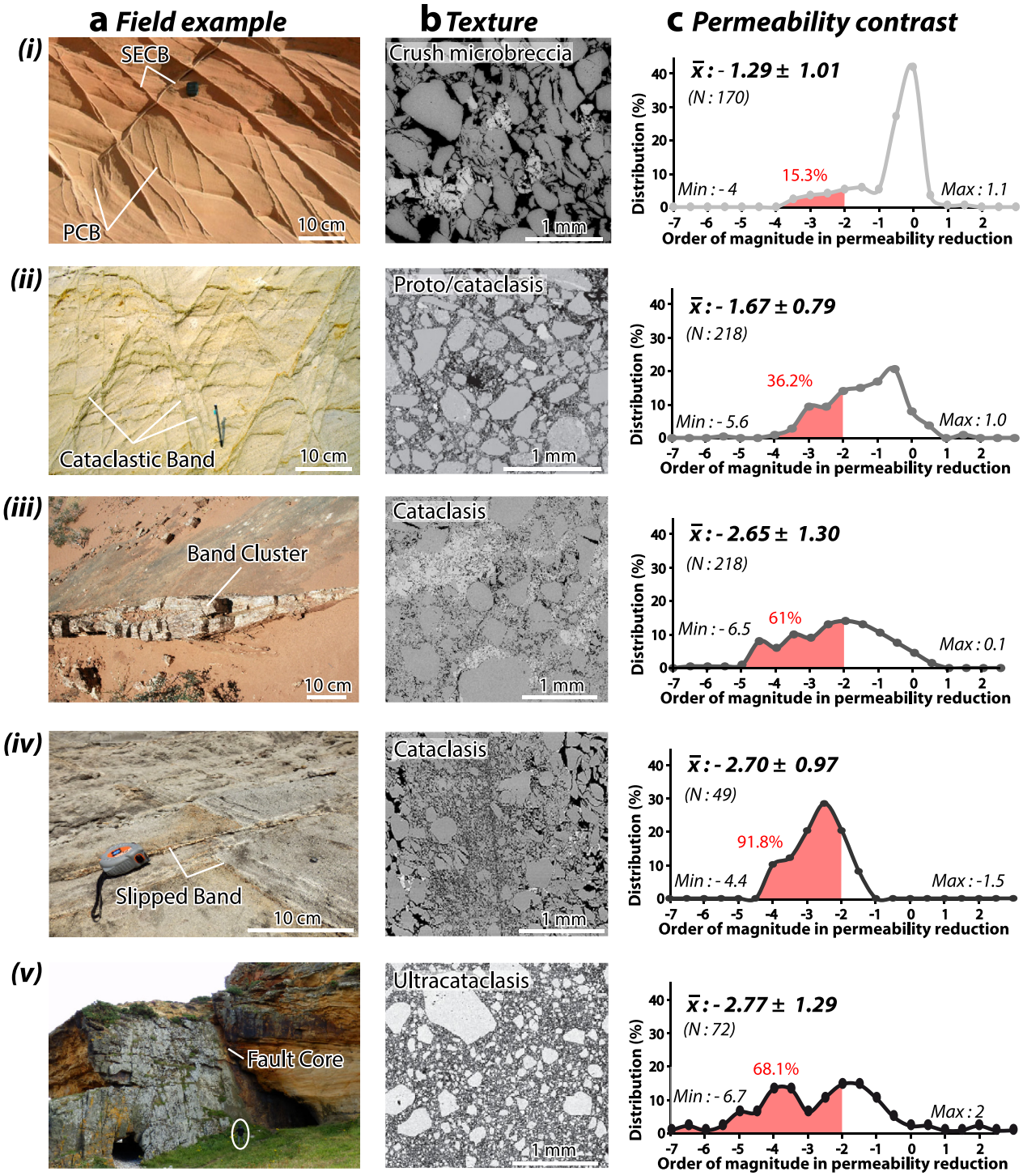


**Fig. 2.** (a) Field examples, (b) SEM photomicrographs of band texture, and (c) graphs of permeability contrast distribution. (i) Pure and shear-enhanced compaction bands (PCB and SECB) showing crush microbreccia (Buckskin Gulch, USA and Provence, France). (ii) Individual cataclastic bands of proto-to cataclastic texture (Provence, France and Eisenstadt-Sopron Basin, Austria (Exner and Tschegg, 2012)). (iii) Cluster of bands showing cataclastic texture (San Rafael Desert, USA and Provence, France). (iv) Slipped bands of cataclastic texture (Pismo Basin, USA and Sinaï, Egypt (Tueckmantel et al., 2010)). (v) Fault cores showing ultracataclastic texture (Moray Firth, Scotland and Provence, France (Saillet and Wibberley, 2013)). Red area corresponds to proportion of bands with more than two orders of magnitude in permeability reduction as compared to host sandstone.

14.8% as fault cores. No PCBs were identified for the normal-fault regime.

### 4.2. Thrust-fault regime

Cataclastic deformation bands formed in the thrust-fault regime show an average permeability contrast of −1.65 ± 1.14 (Fig. 4b). The contrast values range from −4.8 to 1.1 with 26.5% of reverse-sense bands having induced permeability reduction greater than two orders of magnitude (Figs. 4b), i.e. a much smaller number than for the normal-fault regime. Only 6 sites out of 17 (≈35%) have sets of reverse-sense bands involving large permeability decrease. Bands formed include 54.5% as PCBs and SECBs, 27.6% as cataclastic bands, 14.8% as band clusters and 3.1% as slipped bands. No permeability

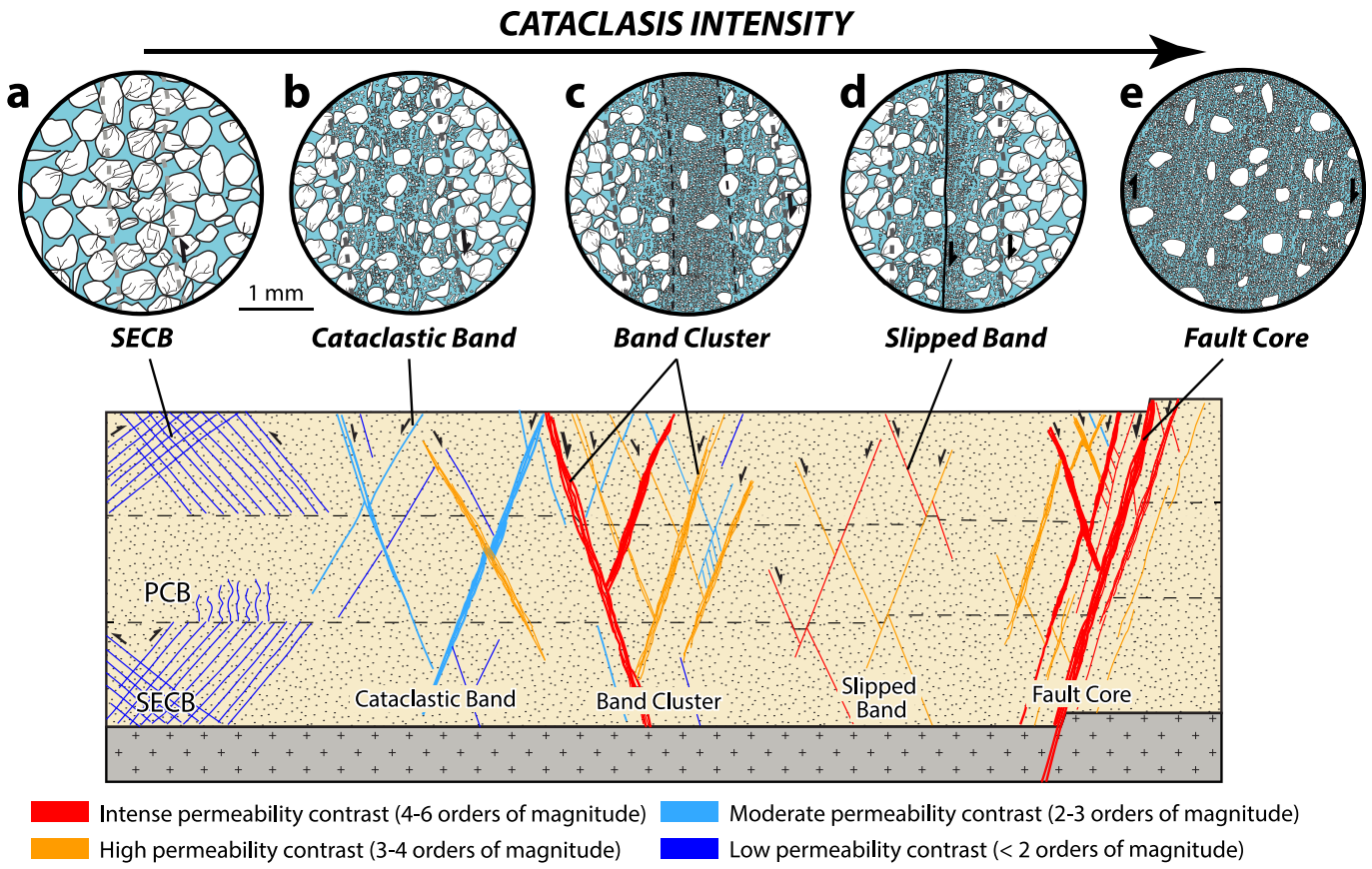


**Fig. 3.** Conceptual model showing the influence of cataclasis intensity on permeability contrast induced by deformation bands and faults in a sandstone reservoir. (a) Pure and Shear-Enhanced Compaction Bands (PCB and SECB). (b) Cataclastic Bands. (c) Band Clusters. (d) Slipped cataclastic Bands. (e) Cataclastic Fault Core. Blue color represents porosity. See main text for explanation. (For interpretation of the references to color in this figure legend, the reader is referred to the web version of this article.)

data have been reported for fault cores from the thrust-fault regime.

### 4.3. Bands related to the presence of a fault

Cataclastic structures formed in sets related to the presence of a fault show an average permeability contrast of $-2.58 \pm 1.38$ (Fig. 4d). This contrast ranges from $-6.7$ to 2 with 52.7% of these bands having induced permeability reduction greater than two orders of magnitude (Fig. 4d). A large majority of the sets (28 out of 37, 75.7%) have bands with structures involving large permeability decrease. Bands of this category comprise 4.3% as bands of low-intensity cataclasis, 31.1% as cataclastic bands, 38.5% as band clusters, 9.3% as slipped bands and 16.7% as fault cores. No PCBs were identified in sets related to the presence of a fault.

### 4.4. Bands formed in area devoid of fault

Cataclastic bands formed in area devoid of large-scale fault show an average permeability contrast of $-1.28 \pm 0.85$ (Figs. 4e), i.e. a much lower number than for the band related to the presence of fault. This contrast ranges from $-4$ to 1.1 with 19.6% of these bands having induced permeability reductions greater than two orders of magnitude (Fig. 4e). 4 out of 12 sets ($\approx$30%) have bands involving large permeability decrease. These bands include 81.5% as PCBs and SECBs and 18.5% as cataclastic bands and band clusters. No permeability data have been reported for slipped bands even if this type of cataclastic structure was observed also in areas devoid of fault (Nevada-Utah, USA; Fossen et al., in press).

### 4.5. Comparison

Statistically, cataclastic bands formed for the normal-fault regime involve more permeability reduction than bands formed for the thrust-fault regime (Figs. 4a, c). The abundance of normal-fault regime bands having permeability reductions greater than two orders of magnitude is more than twice that of the thrust-fault regime, and greater maximum permeability contrasts are also observed for normal-sense structures. Sets containing some bands with large permeability contrast (greater than three orders of magnitude) are also more frequent in the normal-fault regime (Figs. 5a, b). Data obtained in the normal-fault regime come from band sets related to the presence of a fault. Conversely, only a few cases of band sets related to the presence of a fault are observed for the thrust-fault regime.

Cataclastic bands formed in sets related to the presence of a fault generally involve more permeability reduction than bands initiated in areas without fault (Figs. 4d, f). A greater proportion of bands having more than two orders of magnitude of permeability reduction is observed for bands related to localized faults. Sets containing some bands with large permeability contrast are also more frequent when they relate to the presence of a fault. Structures related to faults show more shear, more grain comminution and larger permeability reductions than bands formed in areas devoid of localized faults (Fig. 5i, ii). The major part of band sets related to the presence of a fault is formed under the normal-fault regime even if the few cases observed under the thrust-fault regime show comparable permeability characteristics. Conversely, band sets formed in areas devoid of fault are only found under the thrust-fault regime.

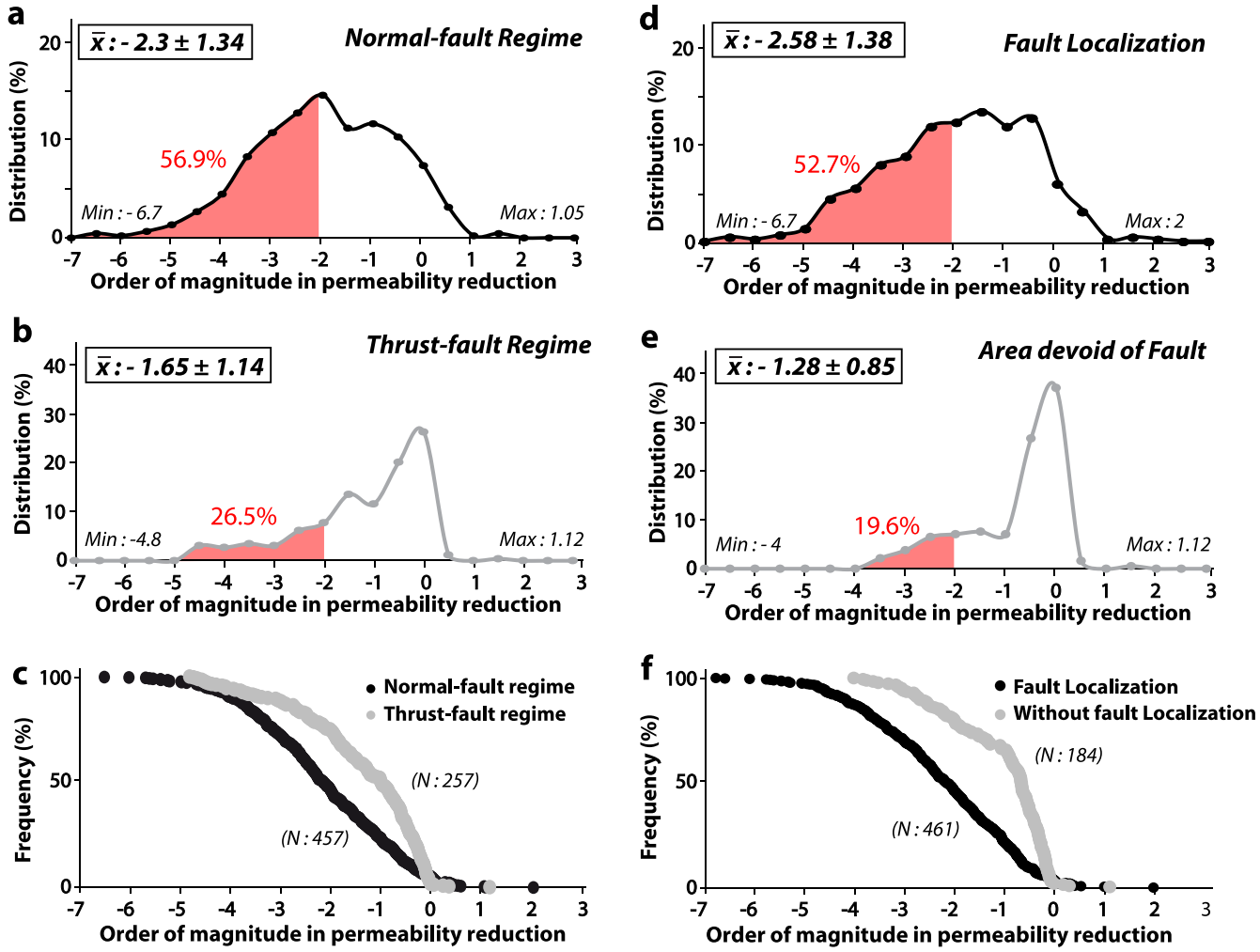


**Fig. 4.** Distribution of permeability contrasts in structures formed in (a) the normal-fault regime; and (b) the thrust-fault regime. (c) Graph showing cumulative frequency of permeability contrast for cataclastic bands and faults formed in normal-fault and thrust-fault regimes. (d) Distribution of permeability contrasts in structures related to the presence of a fault from both regimes. (e) Distribution of permeability contrasts in structures formed in area devoid of fault. (f) Graph showing the frequency of permeability contrast for cataclastic bands and faults formed in sets related to localized fault and sets not related to fault in both regimes.

## 5. Burial depth

Permeability data of cataclastic deformation structures were categorized according to burial conditions (Table 1): (1) shallow-burial depth (<1 km, host sandstones generally un-lithified), (2) moderate-burial depth (1 km–3 km), and (3) deep-burial depth (>3 km, host sandstones generally cemented) (Fig. 6). This designation corresponds generally to the burial depth at time of band formation or, when the timing of band formation is not well constrained, to the maximum burial depth reached by the host sandstone. The influence of tectonic regime and the presence of a fault under shallow and moderate conditions are also analyzed and discussed, although these influences were not investigated for deep burial depth because of the limited amount of data available for these conditions (Figs. 7 and 8). See Supplementary Materials for examples of cataclastic bands formed under different burial conditions (field data and photomicrographs) (Fig. A2).

### 5.1. Shallow burial

Cataclastic structures formed at shallow burial depths show an average permeability contrast of −1.74 ± 1.42 (Fig. 6a). This contrast ranges from −6 to 1.1 with only 24.2% of these bands having induced permeability reductions greater than two orders of magnitude (Fig. 6a). However, 8 sets out of 18 (~44%) have structures involving large permeability decrease (greater than three orders of magnitude). 46.4% of the bands are PCBs and SECBs, 14% are cataclastic bands, 23.4% are band clusters, and 16.2% are fault core elements. No permeability data were reported on slipped bands related to shallow-burial conditions.

### 5.2. Moderate burial

Cataclastic structures formed at moderate-burial depths show an average permeability contrast of −2.51 ± 0.99 (Fig. 6b). This contrast ranges from −6.5 to 0.5 with 64.3% of these bands having induced permeability reduction greater than two orders of magnitude (Fig. 6b). A large majority of sets (15 on 20, ~75%) have bands involving large permeability decrease. These bands include 12.8% as PCBs and SECBs, 43.1% as cataclastic bands, 21.7% as band clusters, 13.5% as slipped bands and 9% as fault cores.

### 5.3. Deep burial

Cataclastic structures found at deep burial depths show an average permeability contrast of −1.89 ± 1.13 (Fig. 6c). This contrast

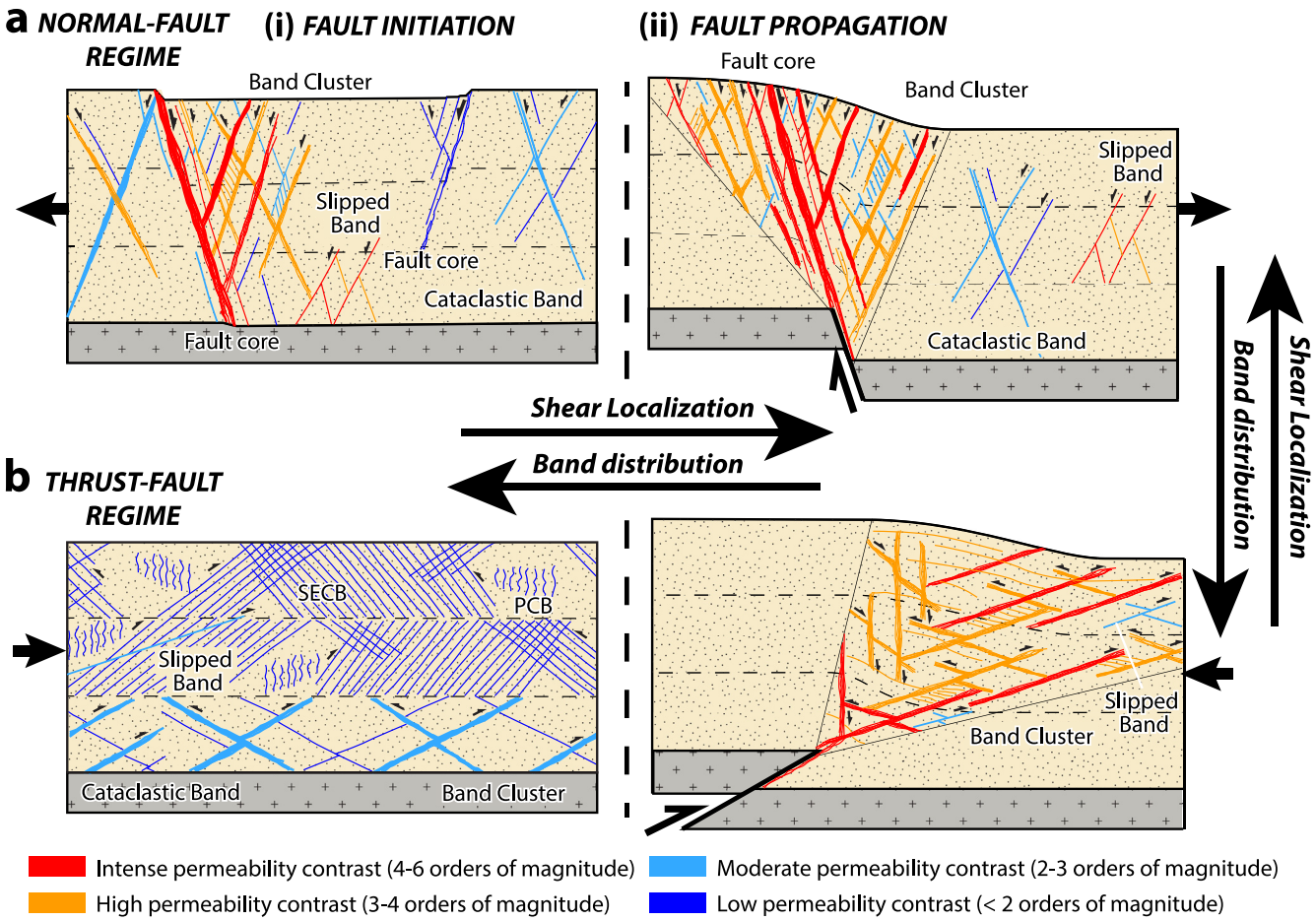


**Fig. 5.** Conceptual models showing the influence of tectonic regime and the presence of a fault on permeability contrast induced by deformation bands. (a) Normal-fault regime. (b) Thrust-fault regime. Both figures illustrate (i) Fault initiation (or area devoid of large-scale fault). (ii) Fault propagation.

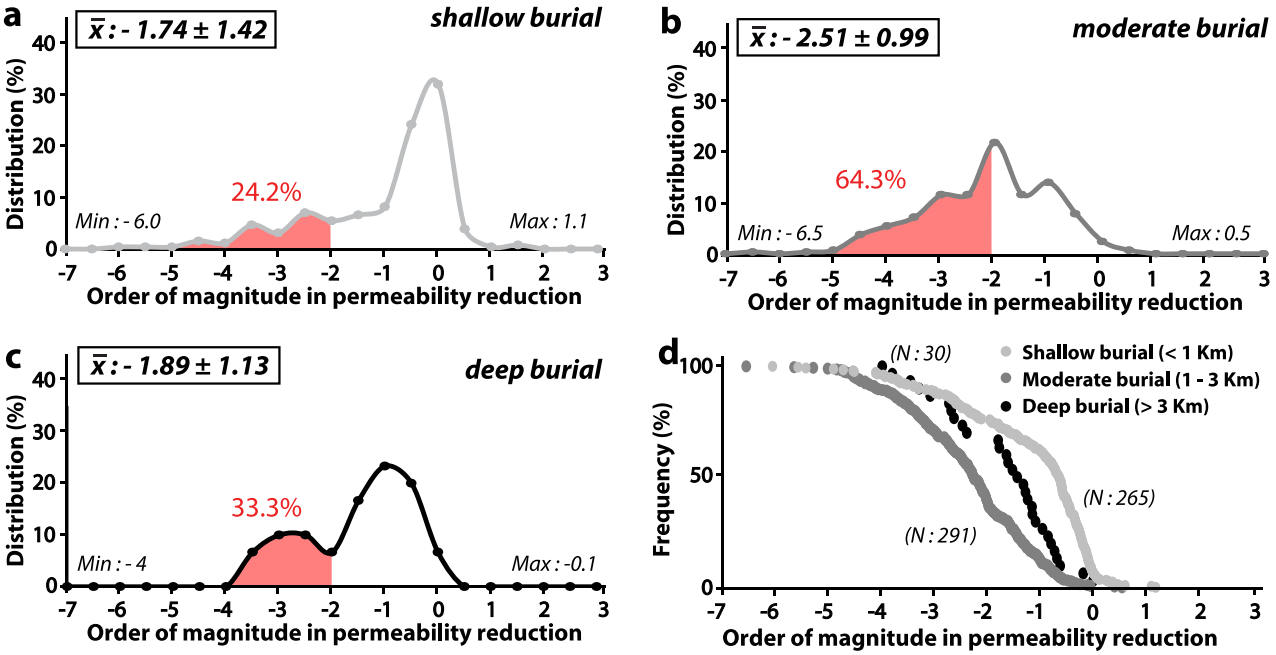


**Fig. 6.** (a) Distribution of permeability contrasts in cataclastic structures formed at shallow burial depths (<1 km). (b) Distribution of permeability contrasts in cataclastic structures formed at moderate burial depths (1 km - 3 km). (c) Distribution of permeability contrasts in cataclastic structures found at deep burial conditions (>3 km). (d) Graph showing the frequency of permeability contrast for cataclastic bands and faults formed at shallow, moderate and deep burial depths.

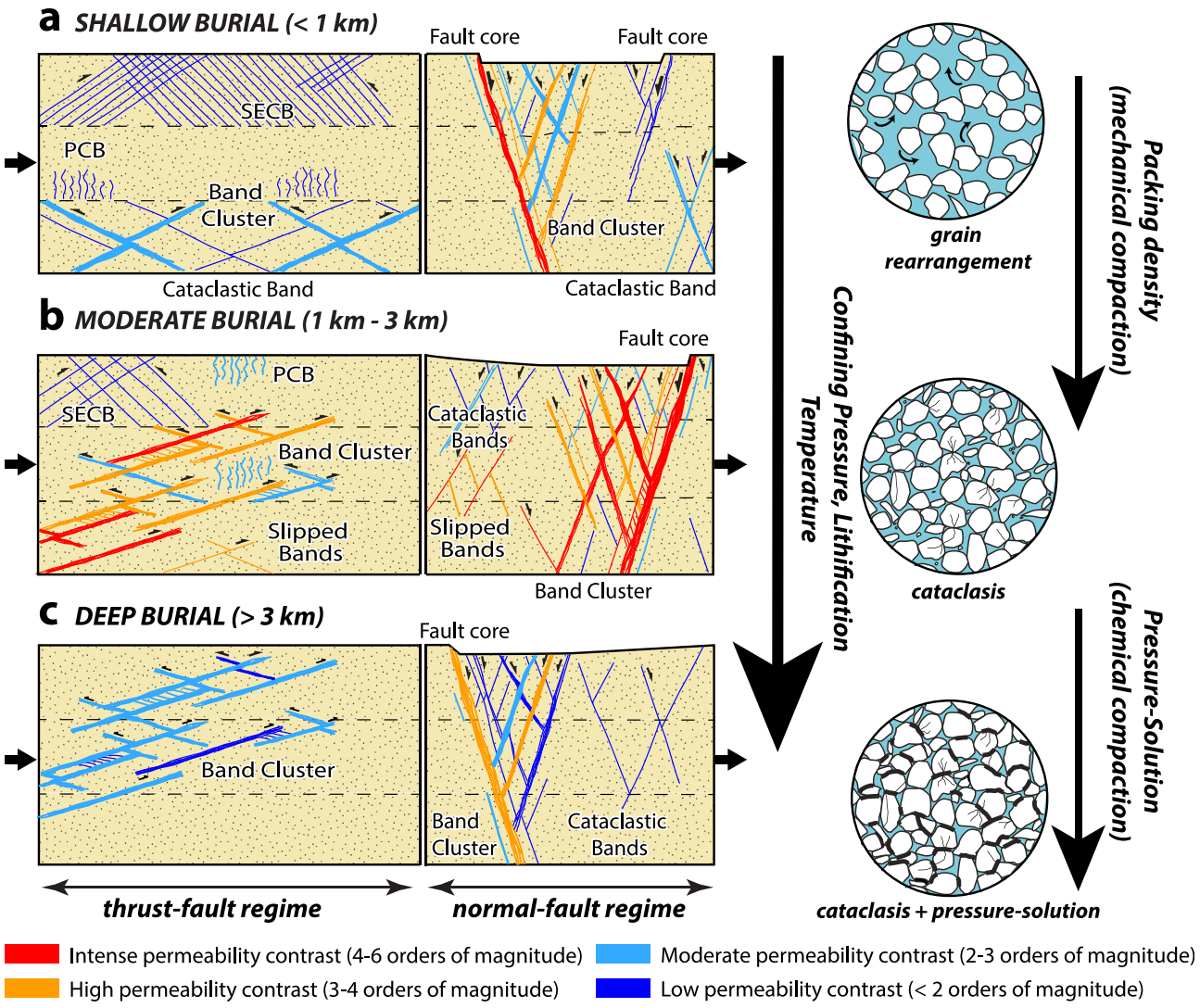


**Fig. 7.** Conceptual models showing the influence of burial depth on permeability contrast induced by cataclastic deformation bands and faults. (a) Shallow burial depth. (b) Moderate burial depth. (c) Deep burial depth.

ranges from −4 to −0.1 with 33.3% of these bands having induced permeability reductions greater than two orders of magnitude (Fig. 6c). Only 3 out of 9 of band sets (~33%) have structures involving large permeability decrease. Few data are available for deep burial conditions (N: 30), but they are all cataclastic bands or clusters showing pressure-solution in addition to cataclasis.

### 5.4. Comparison

Cataclastic bands formed at moderate burial depths involve greater permeability reduction than bands initiated at shallow burial depths (Figs. 6a, b). Greater than two times the proportion of bands has permeability decreases greater than two orders of magnitude for moderate burial as compared to shallow burial conditions. Sets containing some bands with large permeability contrast (greater than three orders of magnitude) are also more frequent at moderate burial depths. Shear bands showing intense cataclasis (band cluster, slipped bands and fault cores) are abundant at moderate burial depths and less common in shallow conditions where bands with less cataclastic deformation are frequently observed (Figs. 7a, b). This influence of burial depth on permeability contrast remains valid regardless of tectonic regime or the presence of localized faults (Figs. 7 and 8). The larger permeability reduction in structures related to the normal-fault regime seems to only apply to shallow burial depths (Fig. 8ai), whereas no clear difference is identified between permeability data of bands formed in both tectonic regimes under moderate burial depths (Fig. 8bi). The larger permeability reduction observed in bands formed in sets related to the presence of a fault remains valid for any burial depth condition (Fig. 8ii).

## 6. Host sandstone porosity

Permeability data of cataclastic deformation structures were classified as a function of the current host sandstone porosity for bands found in: (1) low-porosity (<15%), (2) intermediate-porosity (15%–25%), and (3) high-porosity sandstones (>25%) (Fig. 9 and Table 2). However, the porosity of a host sandstone can change after deformation bands formation, particularly if diagenesis has not or only partly occurred. Any analysis about the influence of host sandstone porosity on band permeability should therefore be considered with care. The influence of tectonic regime, presence of a fault and (shallow and moderate) burial depth within sandstones of different intermediate and high porosities was also considered.

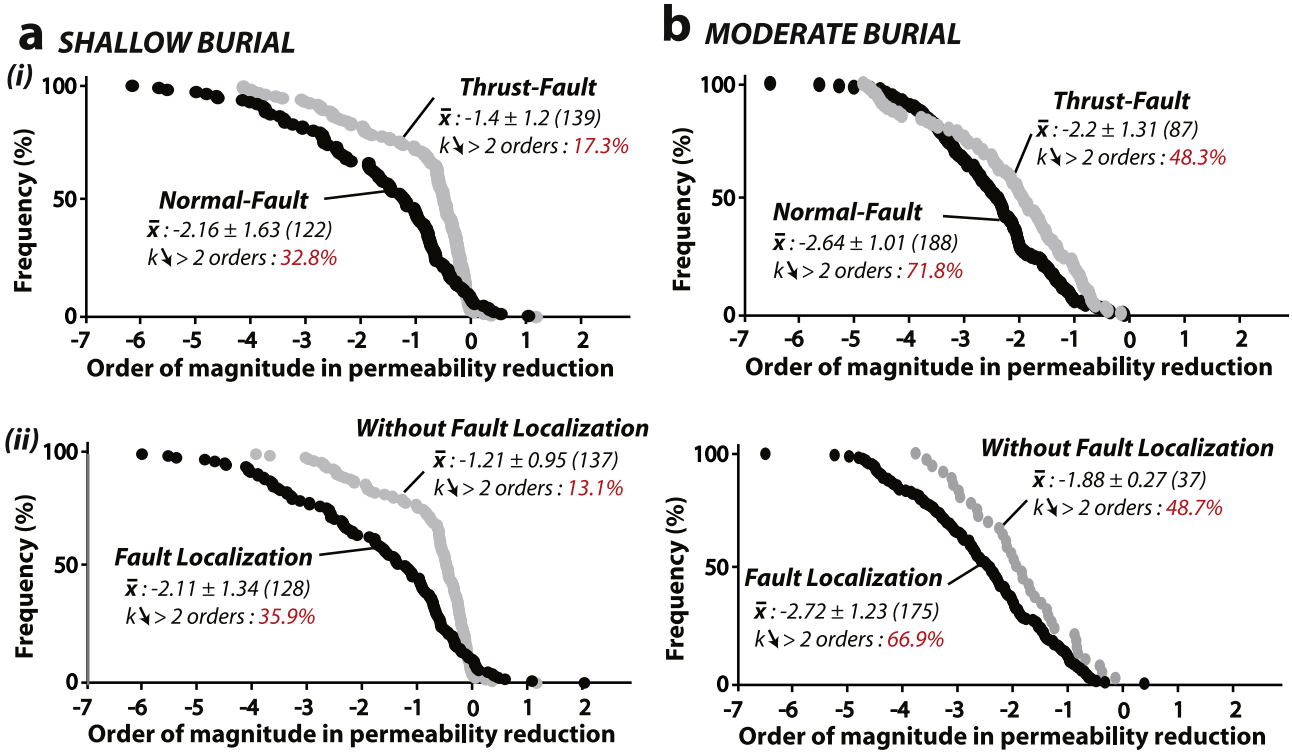


**Fig. 8.** Graphs showing the frequency of permeability contrast for cataclastic bands formed at: (a) shallow burial depth and (b) moderate burial depth, under (i) different tectonic regimes and (ii) related or not to the presence of fault.

However, these influences were not investigated for low-porosity sandstones because of the limited amount of data available for them (Figs. 10 and 11). See Supplementary Materials for examples of cataclastic bands formed in sandstones of different porosity (field data and photomicrographs) (Fig. A3).

### 6.1. Low-porosity sandstone

Cataclastic structures found in low-porosity sandstones show an average permeability contrast of −1.83 ± 1.30 (Fig. 9a). This contrast ranges from −5 to 2 with 45.2% of these bands having induced

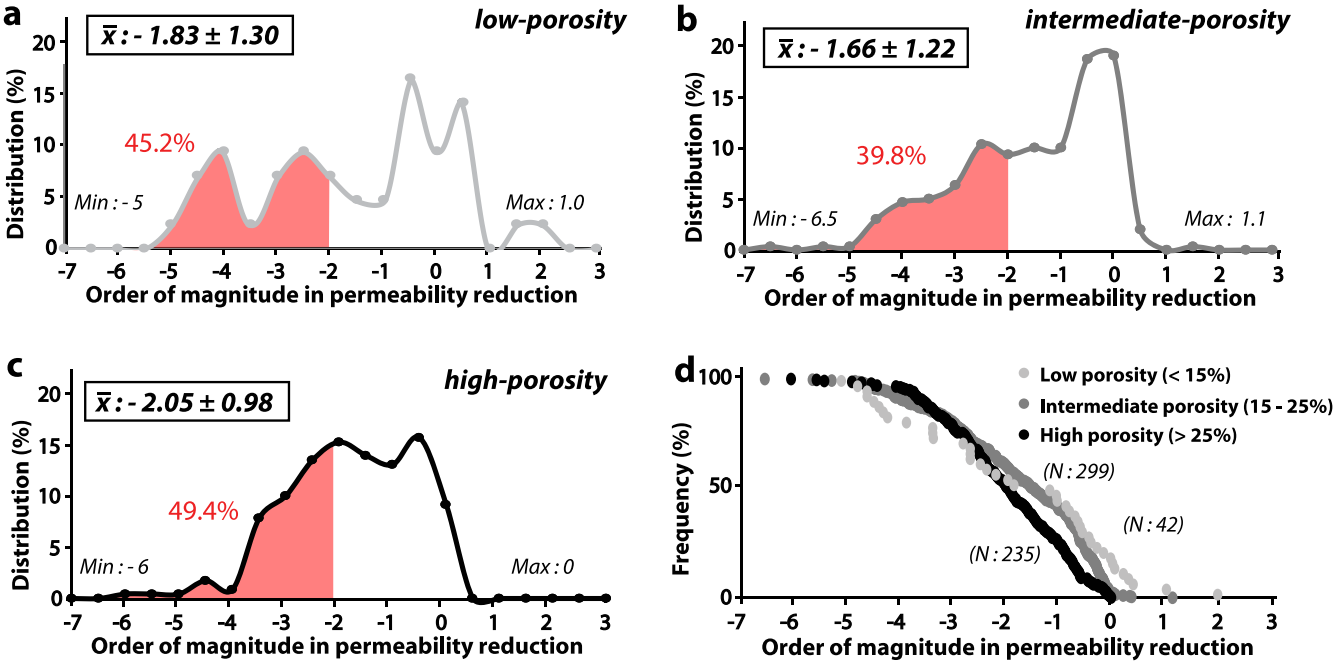


**Fig. 9.** (a) Distribution of permeability contrasts in bands formed in low-porosity sandstones (<15%). (b) Distribution of permeability contrasts in bands and faults formed in intermediate-porosity sandstones (15%–25%). (c) Distribution of permeability contrasts in bands and faults formed in high-porosity sandstones (>25%). (d) Graph showing the frequency of permeability contrast for cataclastic structures formed in sandstones of low, intermediate and high porosity.

permeability reductions greater than two orders of magnitude (Fig. 9a). Only 5 analyzed sandstone units out of 14 (35.7%) have sets with bands involving a large permeability decrease (greater than three orders of magnitude). These bands include 47.6% as cataclastic bands, 16.7% as band clusters, and 35.7% as fault cores. No PCBs and SECBs were identified in low-porosity sandstones.

### 6.2. Intermediate-porosity sandstone

Cataclastic structures found in intermediate-porosity sandstones show an average permeability contrast of −1.66 ± 1.22 (Fig. 9b). The contrast values range from −6.5 to 1.1 with 39.8% of these bands having induced permeability reduction greater than two orders of magnitude (Fig. 9b). Only 22 analyzed sandstone units out of 83 (~26.5%) have sets of bands involving large permeability decrease. Intermediate-porosity sandstone bands include 38.7% as PCBs and SECBs, 26.4% as cataclastic bands, 20.2% as band clusters, 6.9% of slipped bands and 7.9% as fault cores.

### 6.3. High-porosity sandstone

Cataclastic structures found in high-porosity sandstones show an average permeability contrast of −2.05 ± 0.98 (Fig. 9c). This contrast ranges from −6 to 0 with 49.4% of these bands having induced permeability reduction greater than two orders of magnitude (Fig. 9c). Only 19 analyzed sandstone units out of 62 (~31%) have sets of bands with bands involving large permeability decrease. Bands include 14.9% as PCBs and SECBs, 39.6% as cataclastic bands, 26.8% as band clusters, 9.8% as slipped bands and 8.9% as fault cores.

### 6.4. Comparison

Cataclastic bands found in host sandstones of low-porosity involve greater average permeability reduction but slightly less maximum permeability contrast than bands from intermediate and high-porosity sandstones (Figs. 9 and 10). Only cataclastic bands and clusters or fault cores are described in low-porosity sandstones and would be expected to involve larger permeability reduction. However, low-porosity sandstones with cataclastic deformation bands show quartz overgrowths in both bands and host sandstones, which limits the permeability contrast (Fig. 10a). The relatively small data set obtained for such bands does support the general impression that this texture is not favorable to cataclastic deformation.

Less average permeability reduction is observed in bands formed in intermediate-porosity sandstones than for bands formed in high-porosity ones (Figs. 9b, c). However, similar maximum permeability contrasts, proportion of bands inducing more than two orders of magnitude in permeability reduction, and proportion of band sets containing bands of low-permeability (more than three orders of magnitude) are observed for intermediate and high-

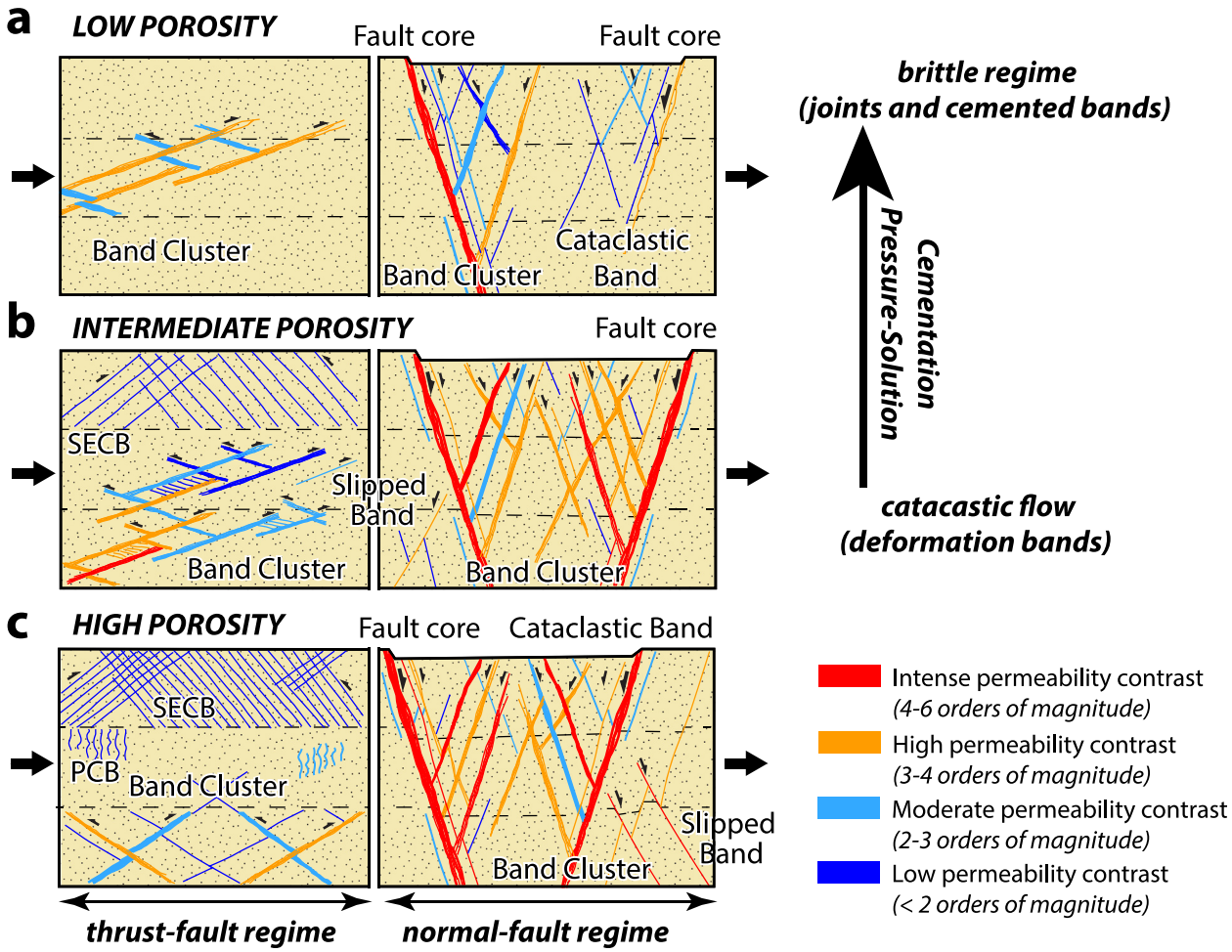


**Fig. 10.** Conceptual models showing the influence of host sandstone porosity on permeability contrast induced by cataclastic deformation bands. (a) Low-porosity. (b) Intermediate-porosity. (c) High-porosity.

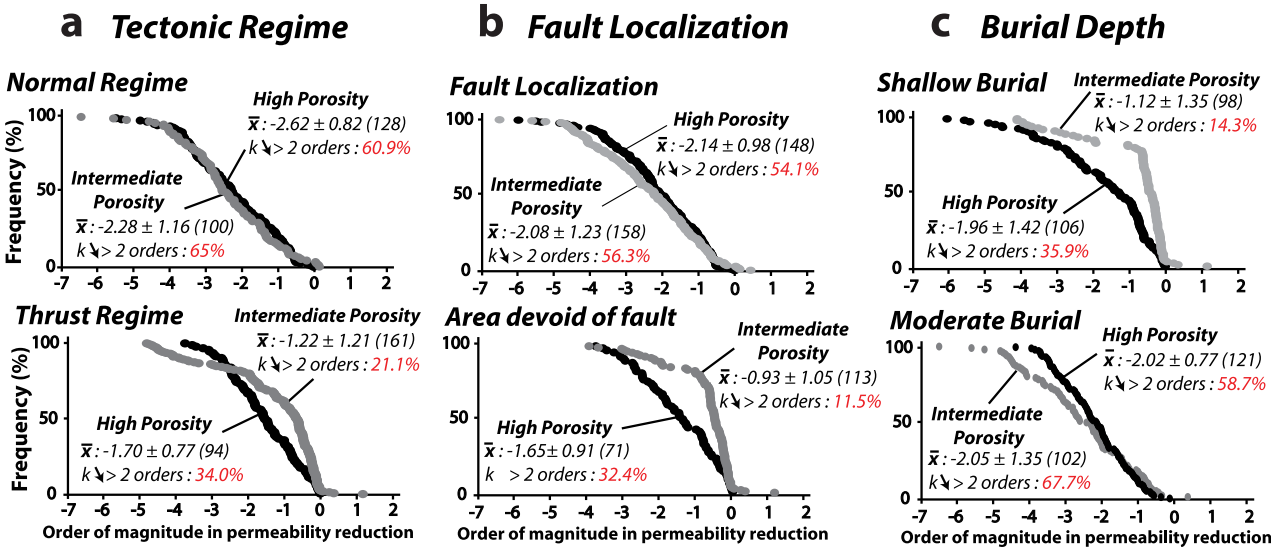


**Fig. 11.** Graphs showing cumulative frequency of permeability contrast for cataclastic bands formed in sandstones of various porosity for: (a) different tectonic regime, (b) presence of fault, (c) and burial depths. Permeability data of structures formed in low-porosity sandstones and deep-burial depth are not represented on these graphs because of the limit amount of data available and probably not representative of these conditions.

porosity sandstones (Figs. 9b, c). Similar permeability reductions are also observed for bands formed in both intermediate and high-porosity sandstones under the normal-fault regime, in area of localized fault and under moderate burial depth, whereas lower permeability reductions are observed for bands formed in intermediate-porosity sandstones under the thrust-fault regime, in area devoid of fault and in moderate burial depth (Fig. 11). All types of cataclastic structures are observed in both host materials, but a slightly greater proportion of the less cataclastic structures is observed in intermediate-porosity sandstones (Figs. 10b, c). This difference in abundance could explain the average lower permeability contrast calculated for these bands. However, these PCBs and SECBs are generally formed in high-porosity sandstones (Eichhubl et al., 2010; Fossen et al., 2011), and the presence of these structures in intermediate-porosity materials could be due to porosity reductions of host sandstones after the band formation, as for example with SECBs from the Buffington Window, Nevada (example in Appendix A). Even if high porosity of host sandstone appears to be a condition for large permeability decrease in cataclastic deformation bands, especially for the normal-fault regime and in moderate burial depth, no clear influence of host sandstone porosity can be identified.

## 7. Host sandstone grain size and sorting

Permeability data were classified as a function of the host-sandstone grain size and grain sorting in bands formed in: (1) coarse-grained sandstones where the mean grain diameter > 0.375 mm, (2) fine-grained sandstones where the grain diameter < 0.375 mm; (3) well-sorted sandstones, and (4) poorly-sorted sandstones (Fig. 12 and Table 2). Contrary to host sandstone porosity, grain size and grain sorting do not generally change over time, unless cataclastic grain size reduction and overgrowth occur but the resultant textures are commonly detectable, which makes conclusions regarding their potential influence on band permeability more reliable. The influence of tectonic regime, the presence of a fault and burial depth within sandstones of different grain size and sorting were also considered (Figs. 13 and 14). See Supplementary Materials for examples of structures formed in sandstones of different grain size and sorting (field data and photomicrographs) (Fig. A4).

### 7.1. Coarse-grained sandstone

Cataclastic structures formed in coarse-grained sandstones show an average permeability contrast of −1.76 ± 1.26 (Fig. 12a). This contrast ranges from −6 to −1.1 with 42.9% of these bands having induced permeability reduction greater than two orders of magnitude (Fig. 12a). 35% of the band sets (26 analyzed sandstone units out of 75) contains bands involving large permeability decrease (greater than three orders of magnitude). These bands include 23.1% as PCBs and SECBs, 19.9% as cataclastic bands, 33.9% as band clusters, 15.4% as slipped bands and 7.7% as fault cores.

### 7.2. Fine-grained sandstone

Cataclastic structures formed in fine-grained sandstones show an average permeability contrast of −1.65 ± 0.99 (Fig. 12b). This contrast ranges from −6.5 to 0 with 40.7% of these bands having induced permeability reductions greater than two orders of magnitude (Fig. 12b). Only 10 analyzed sandstone units out of 71 (~14%) have sets with bands involving large permeability decrease. These bands include 7.7% as SECBs, 46.9% as cataclastic bands, 22% as band clusters, 2.9% as slipped bands and 20.6% as fault cores. No PCBs were identified in fine-grained sandstones.

### 7.3. Well-sorted sandstone

Cataclastic structures formed in well-sorted sandstones show an average permeability contrast of −1.8 ± 0.98 (Fig. 12d). This contrast ranges from −6.5 to 0.6 with 47% of these bands having induced permeability reductions greater than two orders of magnitude (Fig. 12d). Only 23 analyzed sandstone units out of 95 (~24%) have sets with bands involving large permeability decrease. These bands include 24.9% as PCBs and SECBs, 29.3% as cataclastic bands, 27.3% as band clusters, 5.2% as slipped bands and 13.3% as fault cores.

### 7.4. Poorly-sorted sandstone

Cataclastic structures formed in poorly-sorted sandstones show an average permeability contrast of −1.62 ± 1.24 (Fig. 12e). This contrast ranges from −6 to 2 with 42.9% of these bands showing

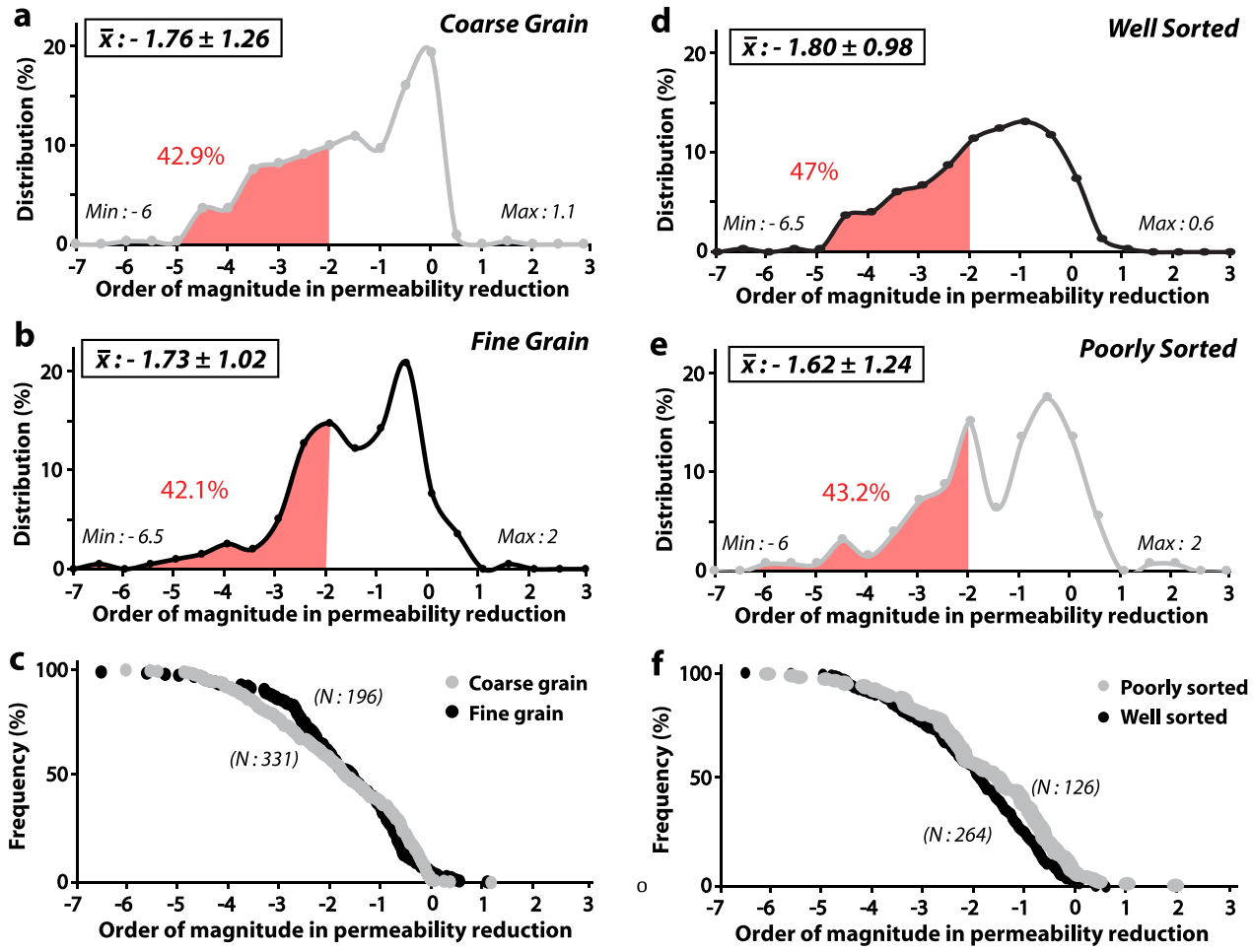


**Fig. 12.** (a) Distribution of permeability contrasts in bands and faults formed in coarse-grained sandstones. (b) Distribution of permeability contrasts in cataclastic structures formed in fine-grained sandstones. (c) Graph showing the frequency of permeability contrast for cataclastic bands and faults formed in fine-grained and coarse-grained sandstones. (d) Distribution of permeability contrasts in structures formed in well-sorted sandstones. (e) Distribution of permeability contrasts in cataclastic structures formed in sets in poorly-sorted sandstones. (f) Graph showing the frequency of permeability contrast for cataclastic bands and faults in well- and poorly-sorted sandstones.

induced permeability reduction greater than two orders of magnitude (Fig. 12e). Only 9 analyzed sandstone units out of 31 (~29%) are band sets with bands involving large permeability decrease. These bands include 12.7% as SECBs, 44.4% as cataclastic bands, 19.1% as band clusters and as 23.8% fault cores. No PCBs and slipped bands were identified in poorly-sorted sandstones.

### 7.5. Comparison

No clear difference in permeability value is observed for bands formed in coarse- and fine-grained sandstones (Figs. 12a, c). The proportion of bands showing permeability reductions greater than two orders of magnitude is also similar in bands formed in both host sandstones, whereas sets containing bands of large permeability reductions are slightly more frequent in coarse material. Band clusters and slipped bands are more abundant in coarse-grained sandstones and involve large grain-comminution and permeability reduction, but also the PCBs and the SECBs which cause only small deformation (Figs. 13a, b). Conversely, fault cores seem more frequent in fine-grained sandstones and should cause intense cataclasis and permeability reduction. Similar maximum permeability contrasts in both coarse and fine-grained sandstones appear consistent with the presence of large-shear structures whatever the grain size of material (Figs. 12a, b). Bands formed in coarse-grained sandstones show larger permeability contrast for the normal-fault regime, in presence of a fault and whatever the burial depths than bands formed in fine-grained sandstones (Fig. 14i). Larger permeability reductions are observed in bands formed in both fine and coarse-grained sandstones for the normal-fault regime as compared to the thrust-fault regime, in presence of a fault and for moderate burial depth as compared to shallow burial conditions (Fig. 14i).

Cataclastic bands formed in well-sorted sandstones involve slightly greater average permeability contrasts and a greater proportion of bands showing permeability reductions >2 orders of magnitude than bands from poorly-sorted sandstones (Figs. 13c, d), but fewer sets containing bands of large permeability decrease (Figs. 12d, f). Well-sorted sandstones show structures with greater permeability contrasts for both normal-fault and reverse-fault regimes, in area devoid of faults and for moderate burial depth (Fig. 14ii). Larger permeability reductions are however observed in bands formed in poorly sorted materials within localized fault and under shallow burial conditions (Fig. 14ii). Hence we see no systematic influence of sorting on cataclastic band permeability from the compiled dataset.

## 8. Discussions

### 8.1. Control of tectonic regime and presence of fault

The normal-fault regime and the presence of fault zones favor the formation of deformation bands and fault cores showing

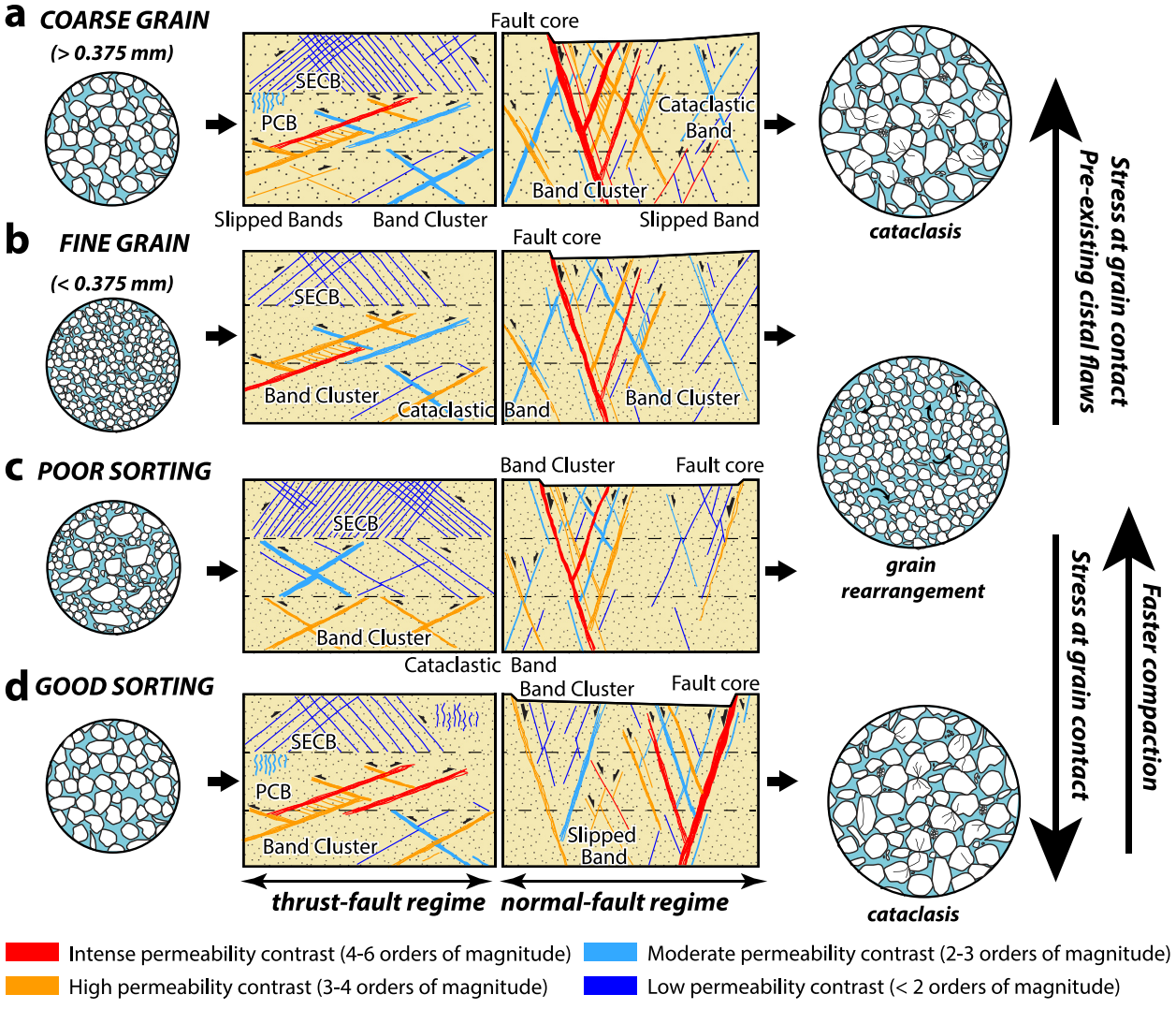


**Fig. 13.** Conceptual models showing the influence of host sandstone characteristics on permeability contrast induced by cataclastic deformation bands and faults. (a) Coarse-grained sandstones. (b) Fine-grained sandstones. (c) Well-sorted sandstones. (d) Poorly-sorted sandstones.

intense cataclasis and large permeability decrease, whereas moderate cataclasis and permeability are recorded in bands formed in the thrust-fault regime and in areas devoid of a fault (Fig. 4). All bands described from normal-fault regimes are related to the process of fault localization, either due to the formation of incipient band clusters or damage zones around well-developed fault cores or slip surfaces (Fig. 5a). Similarly, permeability of fault core elements is only described in structures formed under the normal-fault regime. For similar burial depth, normal-fault and reverse-fault tectonic regimes involve different stress paths that strongly influence the ratio between shear stress and mean-stress at time of band formation (see Soliva et al. (2013) for detailed mechanical explanation of preferential fault localization in the normal-fault regime). The greater shear stress involved in the normal-fault regime favors shear-localization (band cluster) and the initiation of faults (slip-surfaces), whereas the higher mean stress involved in the reverse-fault regime favors the formation of compactional structures such as PCB or SECB (e.g. Ballas et al., 2013; Fossen et al., in press). This difference of stress paths can explain the greater cataclasis intensity and permeability reduction generally recorded in the normal-sense structures compared to reverse-sense ones. However, bands formed in trishear zones to propagating thrusts may also show intense cataclasis and large permeability reductions (Solum et al., 2010; Ballas et al., 2014) (Fig. 5bii). This similarity underscores the influence of large-scale fault reactivation and/or propagation, involving again greater shear stress, on shear localization and permeability reduction in cataclastic deformation bands also in the thrust-fault regime, where fault initiation seems uncommon (Antonellini and Aydin, 1999; Solum et al., 2010). Hence, the tectonic regime and the presence of a fault constitute the major factors controlling permeability contrast induced by cataclastic structures in porous sandstone reservoirs.

### 8.2. Influence of burial depth

The influence of burial depth on band permeability in porous sandstone reservoirs can be explained by the related progressive increase in confining pressure, temperature, and thus host sandstone lithification (mechanical compaction and cementation), although the influence of these parameters can be opposed (Fig. 7). Bands showing limited cataclasis intensity and low permeability reductions are more frequent under shallow and deep burial conditions whereas bands containing intense cataclasis and large permeability reductions are common structures observed under moderate burial conditions (Fig. 6).

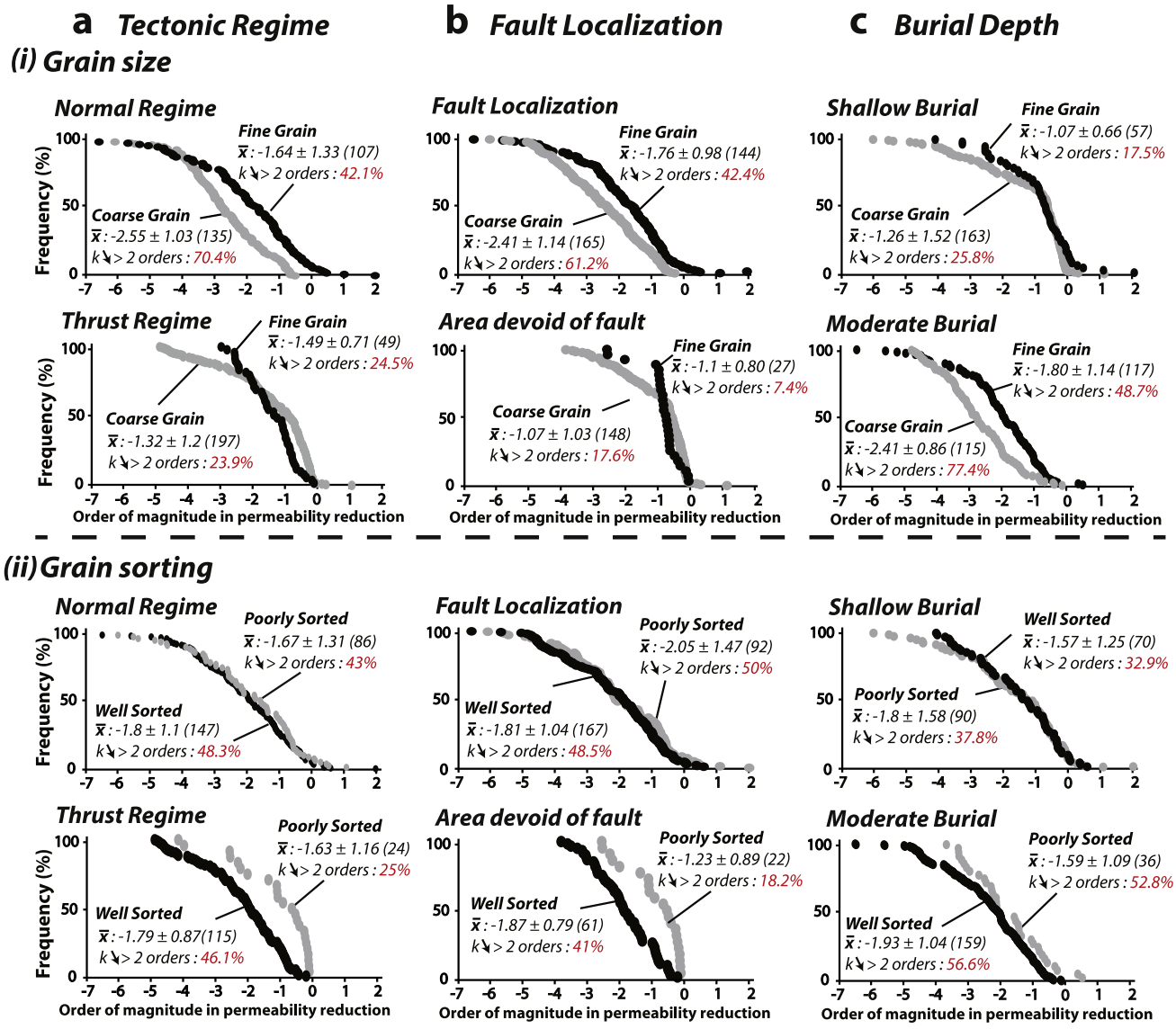


**Fig. 14.** Graphs showing the frequency of permeability contrast for cataclastic bands formed in sandstones as a function of (i) grain size, and (ii) grain sorting, for (a) different tectonic regimes, (b) related or not to the presence of a fault, and (c) various burial depths. Permeability data of structures formed in deep-burial depth are not represented on these graphs because only a few data are available.

Lesser confining pressures favor grain rearrangement and particulate flow, whereas greater confining pressure, generating higher stress concentrations at grain contact points, leads to cataclastic flow (Wong et al., 1997; Mair et al., 2002b; Kristensen et al., 2013). An intensification of cataclasis with the increase of confining pressure should then be observed within the bands (Chuhan et al., 2002), but no quantification of this influence is establish to our knowledge. The evolution of confining pressure in sandstone reservoirs depends on the ratio between horizontal and vertical effective stress ($K_0$), which was estimated to 0.7 by Soliva et al. (2013), but which is susceptible to change with the host sandstone characteristics (Mitchell and Soga, 2005). Hence, a better constrain of the $K_0$ ratio is necessary to predict the influence of confining pressure on deformation band properties in porous sandstones.

Poor lithification of host material, i.e. no cementation and low-packing density generally associated with high porosity, favors grain rearrangement (Antonellini and Pollard, 1995; Skurveit et al., 2013) and therefore the initiation of disaggregation bands (Fisher and Knipe, 1998; Fossen, 2010). Conversely, a high degree of lithification, i.e. high-packing density or cementation, impedes grain rearrangement and favors Hertzian cracking at grain contact points (Rawling and Goodwin, 2003), facilitating bands with more intense cataclasis (Swierczeska and Tokarski, 1998; Labaume and Moretti, 2001; Kaproth et al., 2010; Kristensen et al., 2013).

The high permeability contrasts observed at moderate burial depth, as compared to shallow conditions, can be explained by both higher confining pressure and degree of host sandstone lithification (Fig. 7). Cataclastic bands involving a large permeability decrease are observed in shallow burial conditions (Sidga and Wilson, 2003; Ballas et al., 2012; Saillet et al., 2013), which we infer to mean that other factors can influence cataclasis intensity than burial depth conditions.

### 8.3. Role of host sandstone characteristics

Only limited influences of host sandstone porosity, grain size and grain sorting are revealed by this analysis on cataclastic band type and related permeability reduction (Figs. 9–14). No clear

influence of porosity value is found regarding general permeability reduction in cataclastic deformation bands (Fig. 9). Porosity does not control the intensity of cataclasis when cataclastic deformation bands form. However, a small influence of porosity is observed on permeability for bands formed for the thrust fault regime, where large faults are absent and at shallow burial depths, i.e. greater permeability reduction in bands formed in high-porosity sandstones compared to ones formed in intermediate-porosity sandstones (Fig. 11). This observation implies that the potential influence of host-material porosity depends on the external factors and it only acts as a secondary influencing factor on band permeability.

No significant influence of grain size was identified on the permeability contrasts between cataclastic bands and host sandstones (Figs. 12 and 13a, b). Only slightly greater permeability reductions are observed in the bands formed in coarse-grained sandstones for the normal-fault regime, in areas devoid of a fault and at moderate burial depths (Fig. 14i). This limited influence is consistent with coarse-grain size as condition favorable to cataclasis development, as demonstrated both by field analysis (Eichhubl et al., 2010; Schultz et al., 2010; Balsamo and Storti, 2011; Ballas et al., 2013) and experiment (Wong and Baud, 2012 and references therein) but, similarly to porosity, it only acts as a secondary factor band permeability.

Poor sorting is considered a favorable condition for grain rearrangement (Antonellini and Pollard, 1995), diffuse cataclastic flow (Wang et al., 2008; Cheung et al., 2012) or the formation of bands of low-intensity cataclasis (Ballas et al., 2013; Klimczak and Schultz, 2013), whereas good sorting promotes cataclastic processes (Fowles and Burley, 1994; Antonellini and Aydin, 1995; Solum et al., 2010). The greater stress concentration at Hertzian contacts between certain grains and the faster mechanical compaction of poorly-sorted material, reaching their yielding conditions for lesser stress conditions and leading to diffuse grain cracking, may be responsible for the slightly lower intensity of cataclasis observed in these bands (Skurtveit et al., in press) (Fig. 13b). Good grain sorting constitutes then favorable conditions for greater permeability contrasts within cataclastic structures (Fig. 12). This influence depends however on the presence of large-scale fault or burial depth conditions (Fig. 14ii), so it is only a second-order controlling factor.

## 9. Conclusions

This analysis confirms that permeability decrease is as a function of cataclasis intensity in bands, from low-permeability reduction in crush microbreccia of PCBs and SECBs to high-permeability reduction in cataclasites/ultracataclasites of shear bands (band clusters, slipped bands and fault cores). This analysis emphasizes that cataclasis and permeability reductions are controlled by:

- Tectonic regime and presence of a fault: **Normal-fault regime** and the **presence of a fault**, both for normal and thrust fault regime (i.e. propagation of a basement fault), typically leads to the formation of cataclastic shear bands showing intense cataclasis and high-permeability reduction whereas moderate-permeability reductions are generally recorded in bands formed in the thrust-fault regime and in area devoid of localized fault.
- Burial depth: **Moderate burial depth (1–3 km)** favors the formation of cataclastic bands showing intense cataclasis and high-permeability reduction, whereas smaller permeability reductions are generally observed in bands formed at shallow (<1 km) and deep (>3 km) burial conditions.

The host-sandstone characteristics constitute second-order factors that can influence the permeability of cataclastic bands in specific cases, depending on the external factors. **High porosity**, **coarse grain-size** and **good grain-sorting** can constitute conditions favorable for greater permeability contrasts recorded in cataclastic bands especially for the thrust-fault regime, in areas devoid of a fault and at shallow burial depths.

## Acknowledgments

This work was supported by the Laboratory of Geosciences Montpellier which is gratefully acknowledged. We are grateful to L. Zuluaga for providing permeability data from the San Rafael Reef, and L. De Min and S. Philit for their valuable assistance during field trip. Fabrizio Balsamo, William Dunne and an anonymous reviewer are acknowledged for their comments which greatly improved this manuscript.

## Appendix A

Five new sites were investigated in order to expand the dataset of permeability of cataclastic structures in porous sandstones collected from the literature, all in the western US: (1) San Rafael Desert; (2) Arches Park; (3) San Rafael Reef; (4) Buffington Window; and (5) Pismo Basin. These permeability measurements were done with a portable minipermeameter (Tinyperm-II).

(1) Cataclastic structures at the Arches National Park (Utah) were described by Antonellini and Aydin (1994) and (1995). These structures formed extensional faults related to growth and subsequent collapse of salt anticline (normal-fault regime) and form single bands, band clusters and fault cores. These bands are observed in various sandstone units of different characteristics, but especially in the Navajo and Entrada sandstones, which were buried to around 2.5–3 km depth. Permeability measurements were performed on cataclastic bands and cataclastic band clusters (Figs. Aa and B).

(2) The cataclastic structures of the San Rafael Desert, located close to the Goblin Valley State Park (Utah, USA), were first described by Aydin and Johnson (1978) and more recently by Fossen and Hesthammer (1997) and Johansen and Fossen (2008). These structures are cataclastic normal-faults and band clusters formed in the Cretaceous Entrada Sandstone and accommodate minor NE–SW extension under a maximum burial depth of 2–3 km. Characteristics of the host sandstones are largely variable but permeability measurements were performed on bands formed in porous (25 < < 30%), fine-grained and well sorting sandstone units. Permeability of cataclastic band clusters (Fig. Ab, c) and slipped cataclastic bands were measured (Fig. B).

(3) Cataclastic structures formed along the San Rafael Reef (Utah) have been described by Bump and Davis (2003) and Zuluaga et al. (2014). They are related to the Late Campanian-Eocene Laramide contractional deformation event (reverse-fault regime) and formed in the Navajo and Entrada sandstones under a burial depth of about 2 km. Permeability measurements were mainly done on cataclastic bands and also on a slipped cataclastic band (Fig. Ac), formed in the Entrada Sandstone which shows high porosity (25–30%), fine grain size and good sorting (Table 2).

(4) Cataclastic structures formed in the Jurassic Aztec Sandstone in the Buffington Window (Nevada) were first reported by Engelder (1974) and more recently by Fossen et al. (in press). These structures are distributed shear-enhanced compaction

bands showing low cataclasis intensity (Fig. Ad), related to Sevier thrusting (reverse-fault regime) and formed under shallow conditions (probably less than 1 km). The part of the Aztec Sandstone from where our measurements were taken is generally coarse grained, poorly cemented, and shows porosity ranging from 15% to 25%.

(5) Cataclastic bands and faults described by Antonellini and Aydin (1999) from the Arroyo Grande Oil Field (California) are related to the formation of the Pismo syncline (reverse-fault regime). These structures formed in the Edna Member, which is a poorly consolidated and porous (20%) sandstone. The bands are especially observed in medium to coarse grain size unit. Permeability measurements were mainly done on cataclastic bands but also on band clusters and slipped-bands (Figs. Ae, f and B).

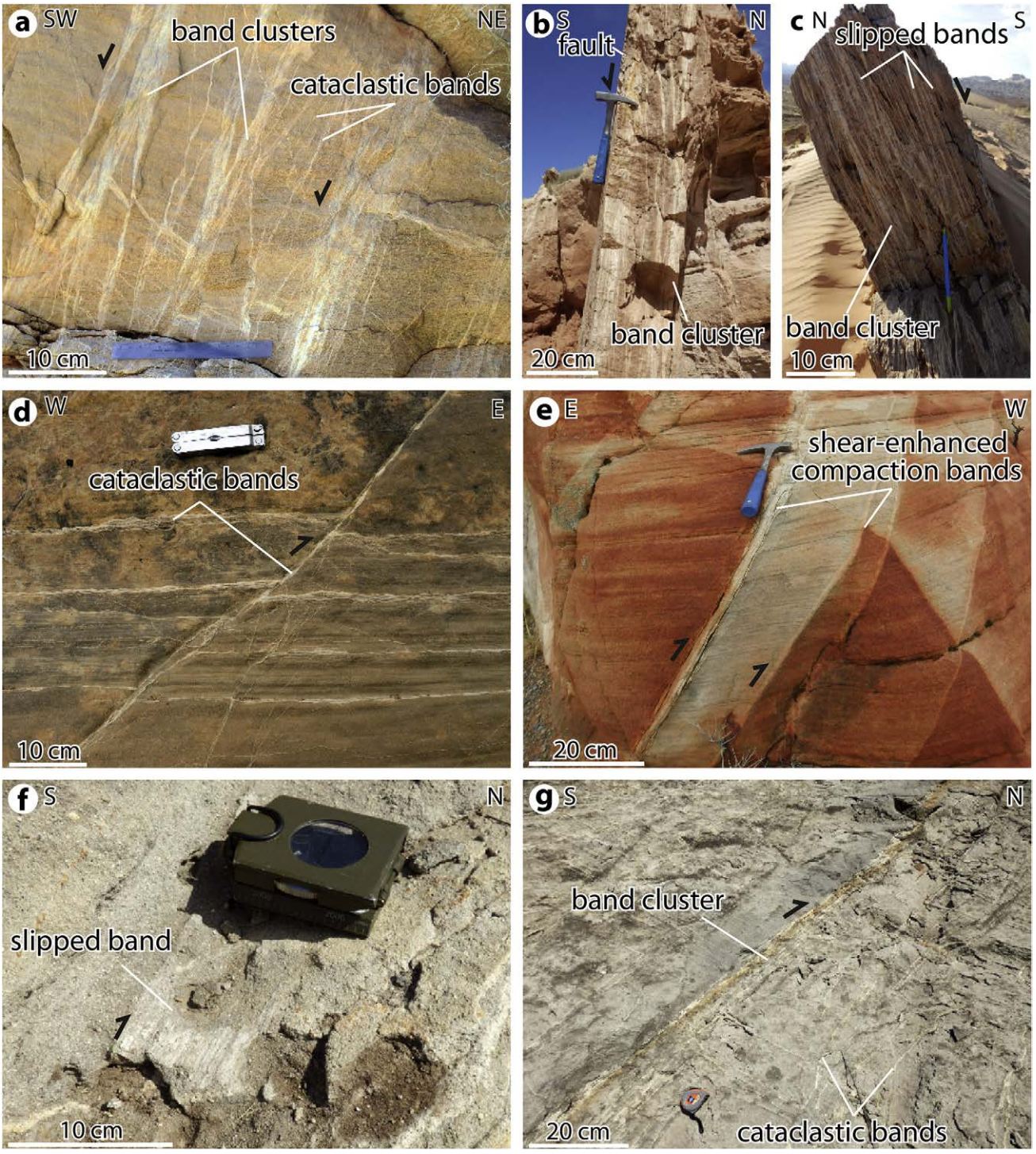


**Fig. A.** (a) Cataclastic bands and band clusters at the Arches National Park. (b) and (c) Band clusters and slipped bands at the San Rafael Desert. (d) Cataclastic bands at the San Rafael Reef. (e) Shear-enhanced compaction bands at the Buffington Window. (f) Slipped cataclastic bands at the Pismo Basin. (g) Cataclastic bands and band cluster at the Pismo Basin.

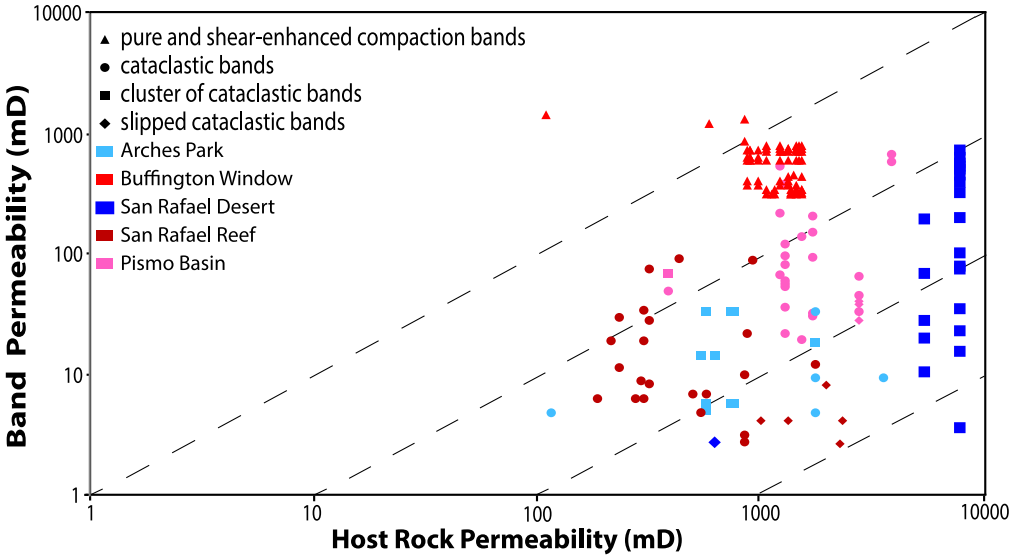


**Fig. B.** Graph showing band permeability vs host-sandstone permeability comparisons for field data collected for this study.

## Appendix B. Supplementary data

Supplementary data related to this article can be found at http://dx.doi.org/10.1016/j.jsg.2015.03.013.

## References


Al-Hinai, S., Fisher, Q.J., Al-Busafi, B., Guise, P., Grattoni, C.A., 2008. Laboratory measurements of the relative permeability of cataclastic fault rocks: an important consideration for production simulation modelling. Mar. Pet. Geol. 25, 473–485.

Antonellini, M.A., Aydin, A., 1994. Effect of faulting on fluid flow in sandstones, petrophysical properties. Am. Assoc. Pet. Geol. Bull. 78, 355–377.

Antonellini, M.A., Aydin, A., Pollard, D.D., 1994. Microstructures of deformation bands in porous sandstones at Arches National Park, Utah. J. Struct. Geol. 16, 941–959.

Antonellini, M.A., Aydin, A., 1995. Effect of faulting on fluid flow in sandstones, geometry and spatial distribution. Am. Assoc. Pet. Geol. Bull. 78, 642–671.

Antonellini, M.A., Pollard, D.D., 1995. Distinct element modeling of deformation bands in sandstone. J. Struct. Geol. 17, 1165–1182.

Antonellini, M.A., Aydin, A., Orr, L., 1999. Outcrop-aided characterization of a faulted hydrocarbon reservoir: Arroyo Grande oil field, California, USA. In: Haneberg, W.C., Mozley, P.S., Moore, J.C., Goodwin, L.B. (Eds.), Faults and Subsurface Fluid Flow in the Shallow Crust, American Geophysical Union Geophysical Monograph, vol. 113, pp. 7–26.

Aydin, A., 1978. Small faults formed as deformation bands in sandstone. Pure Appl. Geophys. 116, 913–930.

Aydin, A., Johnson, A.M., 1978. Development of faults as zones of deformation bands and as slip surfaces in Sandstone. Pure Appl. Geophys. 116, 931–942.

Aydin, A., Borja, R.I., Eichhubl, P., 2006. Geological and mathematical framework for failure modes in granular rock. J. Struct. Geol. 28, 83–98.

Aydin, A., Ahmadov, R., 2009. Bed-parallel compaction bands in aeolian sandstone: their identification, characterization and implications. Tectonophysics 479, 277–284.

Ballas, G., Soliva, R., Sizun, J.-P., Benedicto, A., Cavailhes, T., Raynaud, S., 2012. The importance of the degree of cataclasis in shear bands for fluid flow in porous sandstone (Provence, FRANCE). Am. Assoc. Pet. Geol. Bull. 96, 2167–2186.

Ballas, G., Soliva, R., Sizun, J.-P., Fossen, H., Benedicto, A., Skurtveit, E., 2013. Shear-enhanced compaction bands formed at shallow burial conditions; implications for fluid flow (Provence, FRANCE). J. Struct. Geol. 47, 3–15.

Ballas, G., Soliva, R., Benedicto, A., Sizun, J.-P., 2014. Control of tectonic setting and large-scale faults on the basin-scale distribution of deformation bands in porous sandstone (Provence, France). Mar. Pet. Geol. 55, 142–159.

Balsamo, F., Storti, F., 2010. Grain size and permeability evolution of soft-sediment extensional sub-seismic and seismic fault zones in high-porosity sediments from the Crotone basin, southern Apennines, Italy. Mar. Pet. Geol. 27, 822–837.

Balsamo, F., Storti, F., Salvini, F., Silva, A.T., Lima, C.C., 2010. Structural and petrophysical evolution of extensional fault zones in low-porosity, poorly lithified sandstones of the Barreiras Formation, NE Brazil. J. Struct. Geol. 32, 1806–1826.

Balsamo, F., Storti, F., 2011. Size-dependent comminution, tectonic mixing, and sealing behavior of a "structurally oversimplified" fault zone in poorly lithified sands: evidence for a coseismic rupture? Geol. Soc. Am. Bull. 123, 601–619.

Balsamo, F., Storti, F., Gröcke, D.R., 2012. Fault-related fluid flow history in shallow marine sediments from carbonate concretions, Crotone basin, south Italy. J. Geol. Soc. 169, 613–626.

Balsamo, F., Bezerra, F.H.R., Vieira, M.M., Storti, F., 2013. Structural control on the formation of iron-oxide concretions and Liesegang bands in faulted, poorly lithified Cenozoic sandstones of the Paraìba Basin, Brazil. Geol. Soc. Am. Bull. 125, 913–931.

Bésuelle, P., 2001. Evolution of strain localisation with stress in a sandstone: brittle and semi-brittle regimes. Phys. Chem. Earth 26, 101–106.

Brandenburg, J.P., Alpak, F.O., Solum, J.G., Naruk, S.J., 2012. A kinematic trishear model to predict deformation bands in a fault-propagation fold, East Kaibab monocline, Utah. Am. Assoc. Pet. Geol. Bull. 96, 109–132.

Bump, A.P., Davis, G.H., 2003. Late cretaceous early tertiary laramide deformation in the northern Colorado Plateau, Utah and Colorado. J. Struct. Geol. 25, 421–440.

Cheung, C.S.N., Baud, P., Wong, T-f, 2012. Effect of grain size distribution on the development of compaction localization in porous sandstone. Geophys. Res. Lett. 39, L21302.

Chuhan, F.A., Kjeldstad, A., Bjørlykke, K., Høeg, K., 2002. Porosity loss in sand grain crushing–experimental evidence and relevance to reservoir quality. Mar. Pet. Geol. 19, 39–53.

Crawford, B.R., 1998. Experimental fault sealing: shear band permeability dependency on cataclastic fault gouge characteristics. In: Coward, M.P., Daltaban, T.S., Johnson, H. (Eds.), Structural Geology in Reservoir Characterization, Geological Society, London, Special Publications, vol. 127, pp. 27–48.

Du Bernard, X., Eichhubl, P., Aydin, A., 2002. Dilation bands: a new form of localized failure in granular media. Geophys. Res. Lett. 29 (24), 2176.

Eichhubl, P., Hooker, J., Laubach, S.E., 2010. Pure and shear-enhanced compaction bands in Aztec Sandstone. J. Struct. Geol. 32, 1873–1886.

Engelder, J.T., 1974. Cataclasis and the generation of fault gouge. Geol. Soc. Am. Bull. 85, 1515–1522.

Exner, U., Tschegg, C., 2012. Preferential cataclastic grain size reduction of feldspar in deformation bands in poorly consolidated arkosic sands. J. Struct. Geol. 43, 63–72.

Farell, N.J.C., Healy, D., Taylor, C.W., 2014. Anisotropy of permeability in faulted porous sandstones. J. Struct. Geol. 63, 50–67.

Fisher, Q.J., Knipe, R.J., 1998. Fault sealing processes in siliciclastic sediments. In: Jones, G., Fisher, Q.J., Knipe, R.J. (Eds.), Faulting and Fault Sealing in Hydrocarbon Reservoirs, Geological Society, London, Special Publications, vol. 147, pp. 117–134.

Fisher, Q.J., Knipe, R.J., 2001. The permeability of faults within siliciclastic petroleum reservoirs of the North Sea and Norwegian Continental Shelf. Mar. Pet. Geol. 18, 1063–1081.

Fisher, Q.J., Casey, M., Harris, S.D., Knipe, R.J., 2003. Fluid-flow properties of faults in sandstone: the importance of temperature history. Geology 31, 965–968.

Flodin, E.A., Prasas, M., Aydin, A., 2003. Petrophysical constraints on deformation styles in Aztec Sandstone, Southern Nevada, USA. Pure Appl. Geophys. 160, 1589–1610.

Flodin, E., Gerdes, M., Aydin, A., Wiggins, W.D., 2005. Petrophysical properties and sealing capacity of fault rock, Aztec Sandstone, Nevada. Am. Assoc. Pet. Geol. Mem. 85, 197–217.

Fossen, H., Hesthammer, J., 1997. Geometric analysis and scaling relations of deformation bands in porous sandstone from the San Rafael Desert, Utah. J. Struct. Geol. 19, 1479–1493.
Fossen, H., Schultz, R.A., Shipton, Z.K., Mair, K., 2007. Deformation bands in sandstone: a review. J. Geol. Soc. Lond. 164, 755–769.
Fossen, H., Bale, A., 2007. Deformation bands and their influence on fluid flow. Am. Assoc. Pet. Geol. Bull. 91, 1685–1700.
Fossen, H., 2010. Deformation bands formed during soft-sediment deformation: observations from SE Utah. Mar. Pet. Geol. 27, 215–222.
Fossen, H., Schultz, R.A., Torabi, A., 2011. Conditions and implications for compaction band formation in the Navajo Sandstone, Utah. J. Struct. Geol. 33, 1477–1490.
Fossen, H., Zuluaga, L., Ballas, G., Soliva, R., Rotevatn, A., 2015. Contractional deformation of porous sandstone: insights from the Aztec Sandstone in the footwall to the Sevier-age Muddy Mountains thrust, SE Nevada, USA. J. Struct. Geol (in press).
Fowles, J., Burley, S., 1994. Textural and permeability characteristics of faulted, high porosity sandstones. Mar. Pet. Geol. 11, 608–623.
Gibson, R.G., 1998. Physical character and fluid-flow properties of sandstone-derived fault zones. In: Coward, M.P., Daltaban, T.S., Johnson, H. (Eds.), Structural Geology in Reservoir Characterization, Geological Society, London, Special Publications, vol. 127, pp. 83–97.
Harper, T., Moftah, I., 1985. Skin effect and completion options in the Ras Budran reservoir. In: Society of Petroleum Engineers Middle East Oil Technical Conference and Exhibition, SPE Paper 13708, pp. 211–226.
Hesthammer, J., Fossen, H., 2001. Structural core analysis from the Gullfaks area, northern North Sea. Mar. Pet. Geol. 18, 411–439.
Jamison, W.R., Stearns, D.W., 1982. Tectonic deformation of Wingate Sandstone, Colorado National Monument. Am. Assoc. Pet. Geol. Bull. 66, 2584–2608.
Johansen, T.E.S., Fossen, H., Kluge, R., 2005. The impact of syn-kinematic porosity reduction on damage zone architecture in porous sandstone; an outcrop example from the Moab Fault, Utah. J. Struct. Geol. 27, 1469–1485.
Johansen, T.E.S., Fossen, H., 2008. Internal geometry of fault damage zones in interbedded siliciclastic sediments. In: Wibberley, C.A.J., Kurtz, W., Imbert, J., Holdsworth, R.E., Collettini, C. (Eds.), The Internal Structure of Fault Zones: Implications for Mechanical and Fluid-flow Properties, Geological Society, London, Special Publications, vol. 299, pp. 35–56.
Jourde, H., Flodin, E.A., Aydin, A., Durlofsky, L.J., Wen, X.-H., 2002. Computing permeability of fault zones in eolian sandstone from outcrop measurements. Am. Assoc. Pet. Geol. Bull. 86, 1187–1200.
Kaproth, B.M., Cashman, S.M., Marone, C., 2010. Deformation band formation and strength evolution in unlithified sand: the role of grain breakage. J. Geophys. Res. 115, B12103.
Kheem, Y., Sternlof, K., Mukerji, T., 2006. Computational of compaction band permeability in sandstone. Geosci. J. 10, 499–505.
Klimczak, C., Schultz, R.A., 2013. Fault damage zone origin of the Teufelsmauer, Subhercynian Cretaceous Basin, Germany. Int. J. Earth Sci. 102, 121–138.
Kristensen, M.B., Childs, C., Olesen, N.Ø., Korstgård, J.A., 2013. The licrostructure and internal architecture of shear-bands in sand-clay sequences. J. Struct. Geol. 46, 129–141.
Labaume, P., Moretti, I., 2001. Diagenesis-dependence of cataclastic thrust fault zone sealing in sandstones. Example from the Bolivian Sub-Andean Zone. J. Struct. Geol. 23, 1659–1675.
Lothe, A.E., Gabrielsen, R.H., Bjørnevoll Hagen, N., Larsen, B.T., 2002. An experimental study of the texture of deformation bands : effects on porosity and permeability of sandstones. Pet. Geosci. 8, 195–207.
Mair, K., Main, I., Elphick, S., 2000. Sequential growth of deformation bands in the laboratory. J. Struct. Geol. 22, 25–42.
Mair, K., Frye, K.M., Marone, C., 2002a. Influence of grain characteristics on the friction of granular shear zones. J. Geophys. Res. 107 (B10), 2219.
Mair, K., Elphick, S., Main, I., 2002b. Influence of confining pressure on the mechanical and structural evolution of laboratory deformation bands. Geophys. Res. Lett. 29 (10), 1410.
Medeiros, W.E., do Nascimento, A.F., Alves da Silva, F.C., Destro, N., Demétrio, J.G.A., 2010. Evidence of hydraulic connectivity across deformation bands from field pumping tests: two examples from Tucano Basin, NE Brazil. J. Struct. Geol. 32, 1783–1791.
Menéndez, B., Zhu, W., Wong, T-f, 1996. Micromechanics of brittle faulting and cataclastic flow in Berea sandstone. J. Struct. Geol. 18, 1–16.
Mitchell, J.K., Soga, K., 2005. Fundamentals of Soil Behavior, third ed. John Wiley and Sons, p. 577.
Mollema, P.N., Antonellini, M.A., 1996. Compaction bands: a structural analog for anti-mode I cracks in aeolian sandstone. Tectonophysics 267, 209–228.
Ogilvie, S.R., Glover, P.W.J., 2001. The petrophysical properties of deformation bands in relation to their microstructure. Earth Planet. Sci. Lett. 193, 129–142.
Ogilvie, S.R., Orribo, J.M., Glover, P.W.J., 2001. The influence of deformation bands upon fluid flow using profile permeametry and positron emission tomography. Geophys. Res. Lett. 38, 61–64.
Pittman, E.D., 1981. Effect of fault-related granulation on porosity and permeability of quartz sandstones, Simpson Group (Ordovician), Oklahoma. Am. Assoc. Pet. Geol. Bull. 65, 2381–2387.
Rawling, G.C., Goodwin, L.B., 2003. Cataclasis and particulate flow in faulted, poorly lithified sediments. J. Struct. Geol. 25, 317–331.
Rawling, G.C., Goodwin, L.B., 2006. Structural record of the mechanical evolution of mixed zones in faulted poorly lithified sediments, Rio Grande rift, New Mexico, USA. J. Struct. Geol. 28, 1623–1639.
Rotevatn, A., Torabi, A., Fossen, H., Braathen, A., 2008. Slipped deformation bands: a new type of cataclastic deformation bands in Western Sinai, Suez rift, Egypt. J. Struct. Geol. 30, 1317–1331.
Rotevatn, A., Tveranger, J., Howell, J.A., Fossen, H., 2009. Dynamic investigation of the effect of a relay ramp on simulated fluid flow: geocellular modeling of the Delicate Arch Ramp, Utah. Pet. Geosci. 15, 45–58.
Rotevatn, A., Sandve, T.H., Keilegavlen, E., Kolyukhin, D., Fossen, H., 2013. Deformation bands and their impact on fluid flow in sandstone reservoirs: the role of natural thickness variations. Geofluids 1–13.
Rutter, E.H., 1986. On the nomenclature of mode of failure transitions in rocks. Tectonophysics 122, 381–387.
Saillet, E., Wibberley, C.A.J., 2010. Evolution of cataclastic faulting in high-porosity sandstone, Bassin du Sud-Est, Provence, France. J. Struct. Geol. 32, 1590–1608.
Saillet, E., Wibberley, C.A.J., 2013. Permeability and flow impact of faults and deformation bands in high-porosity sand reservoirs: Southeast Basin, France, analog. Am. Assoc. Pet. Geol. Bull. 97, 437–464.
Sammis, C., King, G., Biegel, R., 1987. The kinematics of gouge deformation. Pure Appl. Geophys. 125, 777–812.
Schueller, S., Braathen, A., Fossen, H., Tveranger, J., 2013. Spatial distribution of deformation bands in damage zones of extensional faults in porous sandstones: statistical analysis of field data. J. Struct. Geol. 52, 148–162.
Schultz, R.A., Siddharthan, R., 2005. A general framework for the occurrence and faulting of deformation bands in porous granular rocks. Tectonophysics 411, 1–18.
Schultz, R.A., Okubo, C.H., Fossen, H., 2010. Porosity and grain size controls on compaction band formation in Jurassic Navajo Sandstone. Geophys. Res. Lett. 37, L22306.
Shipton, Z.K., Cowie, P.A., 2001. Damage zone and slip-surface evolution over μm to km scales in high-porosity Navajo sandstone, Utah. J. Struct. Geol. 23, 1825–1844.
Shipton, Z.K., Evans, J.P., Roberson, K.R., Forster, C.B., Snelgrove, S., 2002. Structural heterogeneity and permeability in faulted eolian sandstone: Implications for subsurface modeling of faults. Am. Assoc. Pet. Geol. Bull. 86, 863–883.
Sibson, R.H., 1977. Fault rocks and fault mechanisms. Geol. Soc. Lond. 133, 191–213.
Sidga, J.M., Wilson, J.L., 2003. Are faults preferential flow paths through semiarid and arid vadose zone? Water Resour. Res. 39, 1225.
Skurtveit, E., Torabi, A., Gabrielsen, R.H., Zoback, M.D., 2013. Experimental investigation of deformation mechanisms during shear-enhanced compaction in poorly lithified sandstone and sand. J. Geol. Res. 118, 4083–4100.
Skurtveit, E., Ballas, G., Fossen, H., Torabi, A., Soliva, R., Peyret, M., 2015. Sand textural control on shear-enhanced compaction band development in poorly-lithified sandstone. J. Geol. Resour. Eng. (in press).
Soliva, R., Schultz, R.A., Ballas, G., Taboada, A., Wibberley, C.A.J., Saillet, E., Benedicto, A., 2013. A model of strain localization in porous sandstone as a function of tectonic setting, burial and material properties; new insight from Provence (SE France). J. Struct. Geol. 49, 50–63.
Solum, J.G., Brandenburg, J.P., Naruk, S.J., Kostenko, O.V., Wilkins, S.J., Schultz, R.A., 2010. Characterization of deformation bands associated with normal and reverse stress states in the Navajo Sandstone, Utah. Am. Assoc. Pet. Geol. Bull. 94, 1453–1475.
Sternlof, K., Karimi-Fard, M., Pollard, D.D., Durlofsky, L.J., 2006. Flow and transport effects of compaction bands in sandstone at scales relevant to aquifer and reservoir management. Water Resour. Res. 42, W07425.
Sun, W., Andrade, J.E., Rudnicki, J.W., Eichhubl, P., 2011. Connecting microstructural attributes and permeability from 3D tomographic images of in situ shear-enhanced compaction bands using multiscale computations. Geophys. Res. Lett. 38, L10302.
Swierczewska, A., Tokarski, A.K., 1998. Deformation bands and the history of folding in the Magura nappe, Western Outer Carpathians (Poland). Tectonophysics 297, 73–90.
Taylor, W.L., Pollard, D.D., 2000. Estimation of in situ permeability of deformation bands in porous sandstone, Valley of Fire, Nevada. Water Resour. Res. 36, 2595–2606.
Tindall, S.E., 2006. Jointed deformation bands may not compartimentalize reservoirs. Am. Assoc. Pet. Geol. Bull. 90, 177–192.
Tondi, E., Antonellini, M., Aydin, A., Marchegiani, L., Cello, G., 2006. The role of deformation bands, stylolites and sheared stylolites in fault development in carbonate grainstones of Majella Mountain, Italy. J. Struct. Geol. 28, 376–391.
Torabi, A., Fossen, H., Alaei, B., 2008. Application of spatial correlation functions in permeability estimation of deformation bands in porous rocks. J. Geophys. Res. 113, B08208.
Torabi, A., Fossen, H., 2009. Spatial variation of microstructure and petrophysical propertie along deformation bands in reservoir sandstones. Am. Assoc. Pet. Geol. Bull. 93, 919–938.
Torabi, A., Fossen, H., Braathen, A., 2013. Insight into petrophysical properties of deformed sandstone reservoirs. Am. Assoc. Pet. Geol. Bull. 97, 619–637.
Torabi, A., 2014. Cataclastic bands in immature and poorly lithified sandstone, examples from Corsica, France. Tectonophysics 630, 91–102.
Tueckmantel, C., Fisher, Q.J., Knipe, R.J., Lickorish, H., Khalil, S.M., 2010. Fault seal prediction of seismic-scale normal faults in porous sandstone: a case study from the eastern Gulf of Suez rift, Egypt. Mar. Pet. Geol. 27, 334–350.
Tueckmantel, C., Fisher, Q.J., Manzocchi, T., Skachkov, S., Grattoni, C.A., 2012. Two-phase fluid flow properties of cataclastic fault rocks: implication for $CO_2$ storage in saline aquifers. Geology 20, 39–42.

Underhill, J.R., Woodcock, N.H., 1987. Faulting mechanisms in high-porosity sandstones; New Red Sandstone, Arran, Scotland. In: Jones, M.E., Preston, R.M.F. (Eds.), Deformation of Sediments and Sedimentary Rocks, Geological Society, London, Special Publications, vol. 29, pp. 91–105.
Wang, B., Chen, Y., Wong, T-f, 2008. A discrete element model for the development of compaction localization in granular rock. J. Geophys. Res. 113, B03202.
Wennberg, O.P., Casini, G., Jahanpanah, A., Lapponi, F., Ineson, J., Wall, B.G., Gillespie, P., 2013. Deformation bands in chalk, examples from the Shetland Group of the Oseberg Field, North Sea, Norway. J. Struct. Geology 56, 103–117.
Wibberley, C.A.J., Petit, J.-P., Rives, T., 2007. The mechanics of fault distribution and localization in high-porosity sands, Provence, France. In: Lewis, H., Couples, G.D. (Eds.), The Relationship between Damage and Localization, Geological Society, London, Special Publications, vol. 164, pp. 599–608.
Wong, T-f., David, C., Zhu, W., 1997. The transition from brittle faulting to cataclastic flow in porous sandstones: mechanical deformation. J. Geophys. Res. 102, 33009–33025.
Wong, T-f., Baud, P., 2012. The brittle-ductile transition in porous rock: a review. J. Struct. Geol. 44, 25–53.
Zuluaga, L., Fossen, H., Rotevatn, A., 2014. Progressive evolution of deformation band populations during Laramide fault-propagation folding: Navajo Sandstone, San Rafael Monocline, Utah, U.S.A. J. Struct. Geol. 68, 66–81.